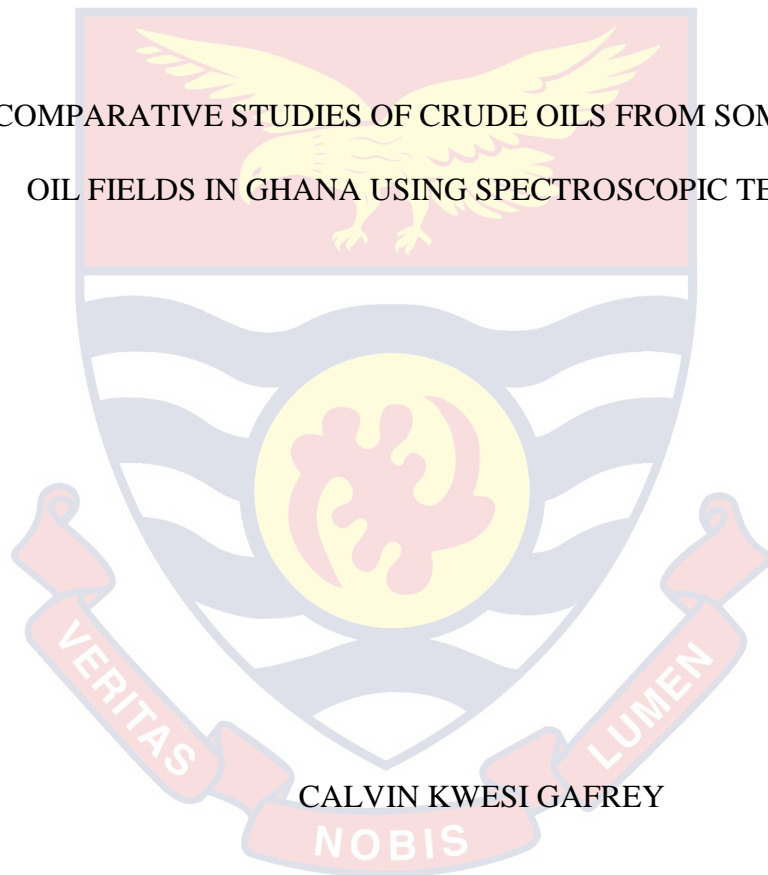


UNIVERSITY OF CAPE COAST

COMPARATIVE STUDIES OF CRUDE OILS FROM SOME SELECTED
OIL FIELDS IN GHANA USING SPECTROSCOPIC TECHNIQUES

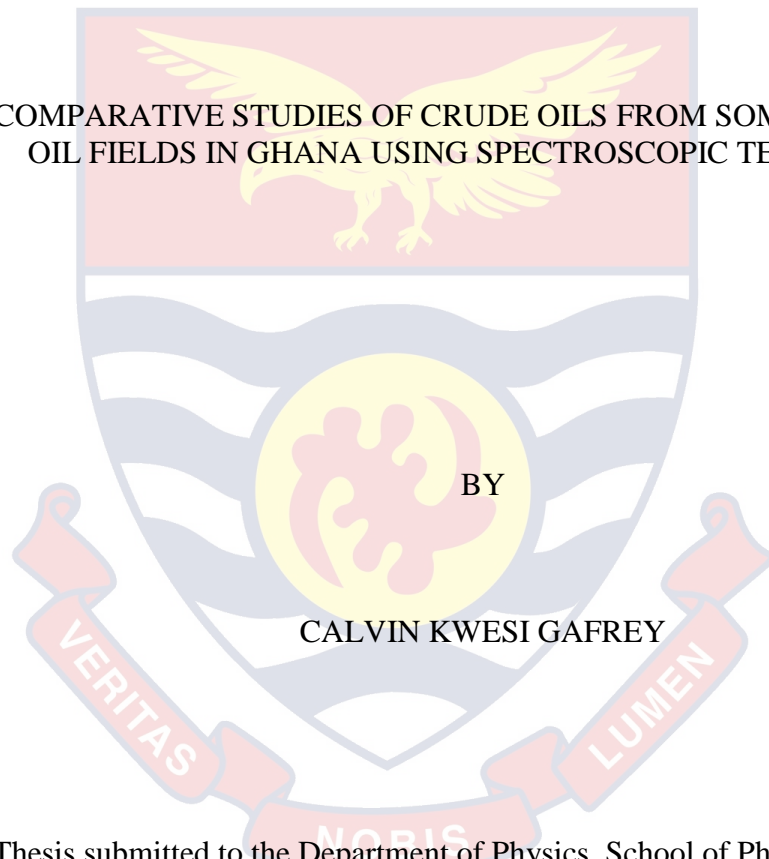


CALVIN KWESI GAFREY

2020

UNIVERSITY OF CAPE COAST

COMPARATIVE STUDIES OF CRUDE OILS FROM SOME SELECTED
OIL FIELDS IN GHANA USING SPECTROSCOPIC TECHNIQUES



BY

CALVIN KWESI GAFREY

Thesis submitted to the Department of Physics, School of Physical Sciences,
College of Agriculture and Natural Sciences, University of Cape Coast, in
partial fulfilment of the requirements for the award of Master of Philosophy
degree in Physics

OCTOBER 2020

DECLARATION

Candidate's Declaration

I hereby declare that this thesis is the result of my own original research and that no part of it has been presented for another degree in this university or elsewhere.

Candidate's Signature: Date:

Name: Calvin Kwesi Gafrey

Supervisors' Declaration

We hereby declare that the preparation and presentation of the thesis were supervised per the guidelines on supervision of thesis laid down by the University of Cape Coast.

Principal Supervisor's Signature: Date:

Name: Prof. George Amoako

Co-Supervisor's Signature: Date:

Name: Prof. Benjamin Anderson

ABSTRACT

Laser-induced fluorescence (LIF), Energy Dispersive X-ray Fluorescence (ED-XRF) and Non-destructive Gamma spectroscopic (NDGS) techniques are the modern spectroscopic techniques used in analysing crude oil samples around the world because of their advantages. There is currently no information on the use of these techniques for the characterisation of crude oils from oil fields in Ghana. This study explored the use of these spectroscopic techniques for characterisation of crude oils from Jubilee, Tweneboa Enyenra Ntomme (TEN) and Saltpond oil fields. LIF, ED-XRF and NDGS techniques were applied on four crude oil samples obtained from these oil fields. Fluorescence spectra obtained, using a continuous wave 405 nm laser as the excitation source, revealed five (5) peak wavelengths after deconvolution. Using Principal Component Analysis (PCA), Hierarchical Clustering Analysis (HCA), and Linear Discriminant Analysis (LDA), the crude oil samples were classified accurately. Using the fluorescence spectra from the ED-XRF sulphur concentrations in the crude oil samples were determined. Based on their Sulphur concentrations, the four crude oil samples were characterised as sweet oils. NDGS was able to identify naturally occurring radionuclides ^{226}Ra , ^{232}Th and ^{40}K . Thus, it is feasible to use LIF, EDXRF and NDGS as simple and straightforward spectrochemical techniques to characterise crude oils from Ghana's oil fields effectively.

KEY WORDS

Crude Oil

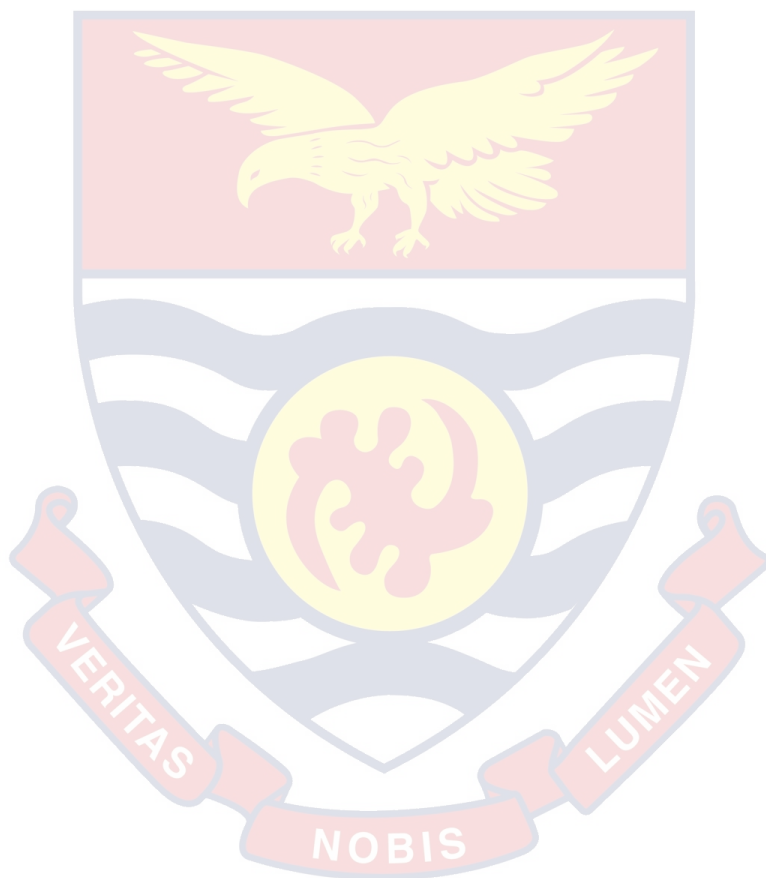
Laser-Induced Fluorescence

Naturally Occurring Radioactive Materials

Peak Deconvolution

Principal Component Analysis

X-ray Fluorescence



ACKNOWLEDGEMENTS

My profound gratitude goes to my Principal Supervisor, Prof. George Amoako for his unflinching supervision to fine-tune this research work. My gratitude also goes to my Co-Supervisor, Prof. Benjamin Anderson for his time and coaching to refine this research work. I am indebted to Dr. Owiredu Gyampo and all staff of the National Nuclear Research Institute, Ghana Atomic Energy Commission, Kwabenya, for their immense help in making this research work a success.

My heartfelt gratitude goes to all lecturers and staff of the Department of Physics especially Prof. Moses Jojo Eghan, Dr. Baah Sefa Ntiri, Dr. Raymond Edziah, Dr. Anthony Twum and Mr. Patrick Mensah Amoah. I am sincerely grateful to all senior and junior colleagues of the Laser and Fibre Optics Centre (LAFOC) especially Dr. Charles Lloyd Amuah, Dr. Peter Osei-Wusu Adueming, Mr. Andrew Huzortey, Mr. Rabbi Boateng and Miss Nana Esi Nyarko.

Finally, a special thank you to Mr. Henry Kwesi-Brown Gafrey, Mr. Samuel Abaku Tetteh-Yemoh, Mr. Robert Wilson, Mr. Anthony Annefi and all who played an important role throughout my studies. You have been such wonderful people and God richly bless you all.

DEDICATION

To my parents Mr. Sammy Lucky Gafrey and Mrs. Bertha Tuapany Gafrey and
Sister Susan Gafrey for their love and support.

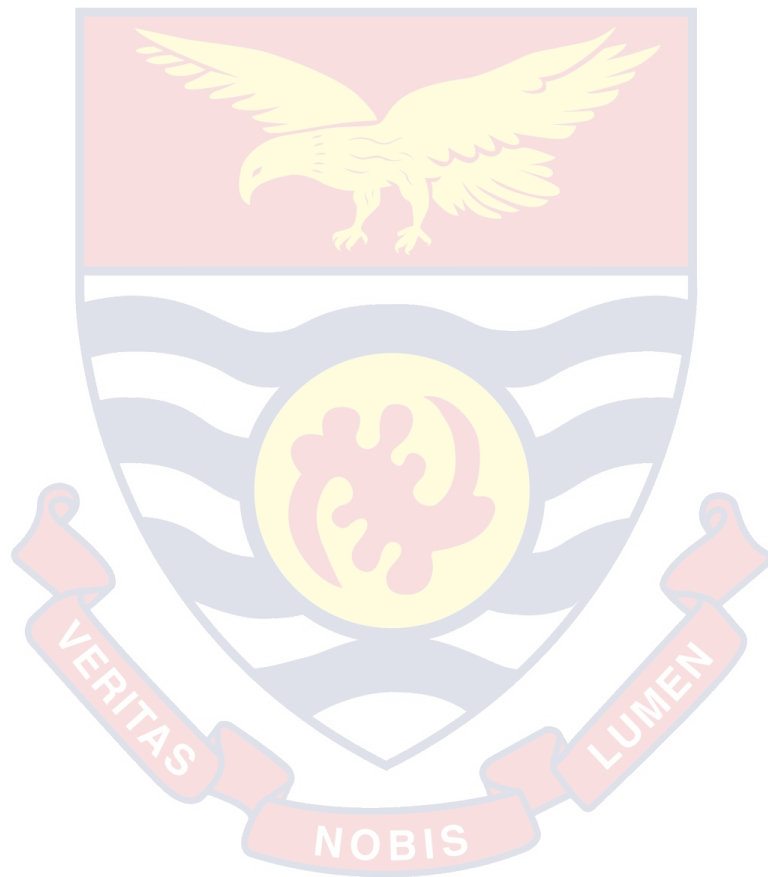


TABLE OF CONTENTS

	Page
DECLARATION	ii
ABSTRACT	iii
KEY WORDS	iv
ACKNOWLEDGEMENTS	v
DEDICATION	vi
LIST OF TABLES	xi
LIST OF FIGURES	xii
LIST OF ABBREVIATIONS	xv
LIST OF SYMBOLS	xviii
CHAPTER ONE: INTRODUCTION	
Background to the Study	1
Research Problem Statement	4
Research Questions	5
Research Objectives	5
The Rationale behind this Study	6
Delimitation	6
Limitation	7
The Organization of the Study	7
Chapter Summary	8
CHAPTER TWO: LITERATURE REVIEW	
Introduction	9
Crude Oil Formation	9
Oil Fields in Ghana	14

Laser-Induced Fluorescence (LIF) Spectroscopy	18
The Fluorescence Process	19
Theory of Fluorescence Emission	19
Data Pre-processing Technique	21
Normalization Methods	22
Peak Deconvolution	23
The Gaussian Function Fitting Methods for Fluorescence Spectra	23
Principal Component Analysis (PCA)	25
Hierarchical Clustering Analysis (HCA)	27
Linear Discriminant Analysis (LDA)	27
LIF Measurement Techniques Used in Petroleum Research	28
Inner Electron Spectroscopy	30
X-ray Emission Spectroscopy	32
Energy Dispersive Spectroscopy	33
The Sensitivity of the System and its Application in Petroleum Research	33
Application of X-ray Spectroscopy	36
Naturally Occurring Radioactive Materials in Petroleum	37
Significance of Assessing NORM presence in Crude Oil in Ghana	39
Chapter Summary	40
CHAPTER THREE: RESEARCH METHODS	
Introduction	41
Samples	41
The Oil Fields	42
Laser-Induced Fluorescence (LIF) Measurement	43
Experimental Set-Up	43

LIF Measurement	45
Data Analysis of LIF Measurement	45
X-ray Fluorescence (XRF) Measurement	46
Experimental Set-Up	46
Scale Calibration of Amptek DPP MCA	48
XRF Measurement	48
Data Analysis of XRF Measurement	50
Gamma Ray Spectrometer Measurement	51
Experimental Set-Up	51
Multichannel Analyser	51
Gamma-Ray Measurement	52
Chapter Summary	55
CHAPTER FOUR: RESULTS AND DISCUSSION	
Introduction	56
Fluorescence Emission of Crude Oil Samples	56
Fluorescence Spectra Deconvolution of Crude Oil Samples	59
Principal Component Analysis (PCA) of the Fluorescence Spectra obtained from Crude Oil Samples	63
Hierarchical Clustering Analysis (HCA) of the Fluorescence Spectra	66
Linear Discriminant Analysis (LDA)	67
Sulphur Concentration	69
Radionuclides from the Crude Oils	70
Chapter Summary	73

CHAPTER FIVE: SUMMARY, CONCLUSIONS AND
RECOMMENDATIONS

Overview	75
Summary	75
Conclusions	77
Recommendations	78
REFERENCES	79



LIST OF TABLES

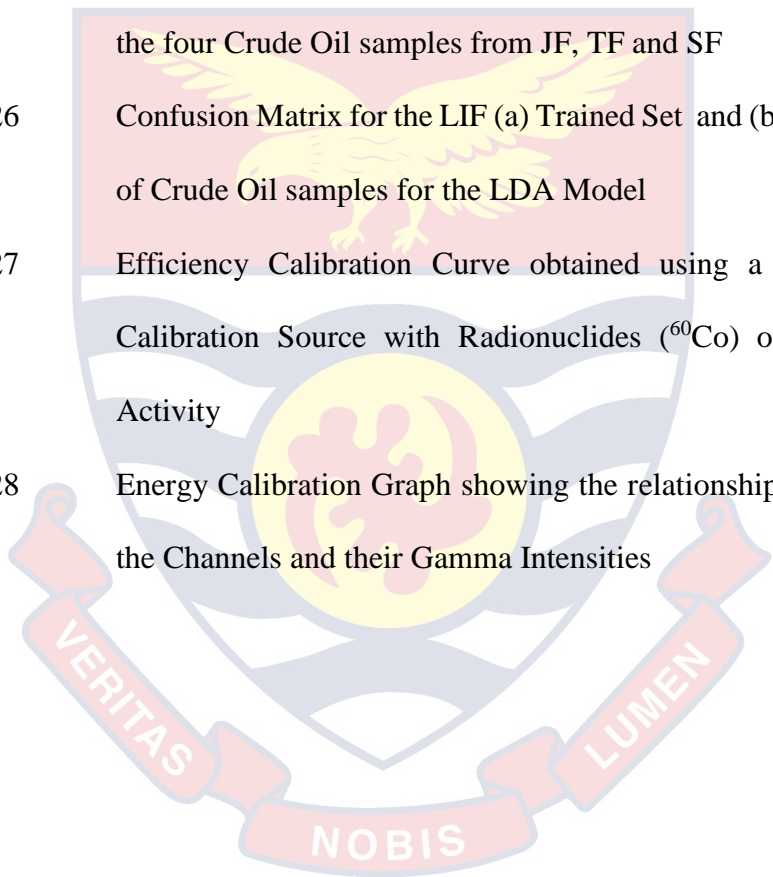
	Page
1 Petroleum Hydrocarbon Composition (Hook, 2009)	11
2 Non-Hydrocarbon Composition of Petroleum (Hook, 2009)	12
3 Elemental Percentage Range (Bawazeer & Zilouchian, 1997)	13
4 Summary of the Crude Oil samples, Oilfield Locations and sample Codes used	42
5 Results of Deconvoluted Fluorescence Spectra for Crude Oil samples from all four (4) Oil Wells	61
6 Average Peak Wavelength Values of Deconvoluted Fluorescence Spectra for Crude Oil samples from JF, TF, SF1 & SF 2 Oil Fields	62
7 Sulphur Concentration Levels of Crude Oil samples	69
8 Activity Concentration of ^{226}Ra and ^{232}Th from JF, TF and SF compared to IAEA Basic Safety Standards (BSS) Exemption Level, 1×10^1 (Bq/g)	72
9 K-40 Activity Concentration obtained in this work compared to IAEA Basic Safety Standards (BSS) Activity for Radionuclides of Natural Origin, 1×10^1 (Bq/g)	73

LIST OF FIGURES

	Page	
1	Map showing the Different Geological sources of Crude Oil that Ghana has	15
2	Saltpond Offshore Field showing the Locations of two Oil Fields	16
3	Geological Locations of the Tweneboa Enyenra Ntomme (TEN) Oil Fields	17
4	A simplified Jablonski Diagram describing the Fluorescence Process	20
5	X-ray Transition of Inner Electron Energy Levels	31
6	Diagram Illustrating Moseley's Law	32
7	Results of Trace Elements found in Saltpond and Jubilee Oil	35
8	Crude Oil samples in bottles obtained from Jubilee, TEN and Saltpond Oil Fields	41
9	Satellite view showing the three Oil Fields with their Geological Positions along the Saltpond and Takoradi Coastal Arches	42
10	Schematic Diagram for the LIF Measurement Set-Up showing the Radiation Source (Diode Laser), the Analyte (Crude Oil), Optical Components (Fibre Probe) and the Detection System (Spectrometer with Filter)	44
11	In-built Mini-X Radiation Source	47
12	AMPTEK EXP-1 X-123 XRF Experimenter Kit showing the Radiation Source (Mini-X-ray Tube) and Spectrometer (X-	

	123) both situated beneath the Radiation Shielding Compartment	47
13	The Shielding Compartment with Safety Plunger showing the Safety Features of the AMPTEK EXP-1 X-123 XRF Experimenter Kit	49
14	Sample Holder in the Shielding Compartment of the AMPTEK EXP-1 X-123 XRF Experimenter Kit showing the Sample-Detector Configuration	50
15	DSPEC Series Multichannel Analyzer (AMETEK ORTEC, U.S.A)	52
16	Marinelli Beaker filled with Crude Oil and Sealed Detector-Beaker Configuration	53
17	DSPEC LF MCA-Computer Configuration	54
18	Unprocessed Relative Fluorescence Spectra of all the Crude Oil samples JF, TF, SF 1 and SF 2 from the four Oil Wells showing the Dominating Spectral Signatures	57
20	Average Normalized Fluorescence Spectra from four Crude Oil samples from four (4) Oil Wells	58
21	Deconvoluted Fluorescence Spectra of (a) JF, (b) TF, (c) SF1 and (d) SF 2 showing the Hidden Peaks	60
22	Number of Principal Components and their Contribution to the Variation in the Data Set Explained Percentagewise	63

23	Loadings Plot from the PCA of the LIF Spectra giving information about the significant sources of Variation in the Data	64
24	Scores Plot for PC1 and PC2 from Principal Component Analysis of the LIF Spectra obtained from the four Crude Oil samples, JF, TF, SF 1 and SF 2	65
25	Dendrogram of the Laser-Induced Fluorescence Spectra of the four Crude Oil samples from JF, TF and SF	66
26	Confusion Matrix for the LIF (a) Trained Set and (b) Test Set of Crude Oil samples for the LDA Model	68
27	Efficiency Calibration Curve obtained using a Standard Calibration Source with Radionuclides (^{60}Co) of Known Activity	70
28	Energy Calibration Graph showing the relationship between the Channels and their Gamma Intensities	71

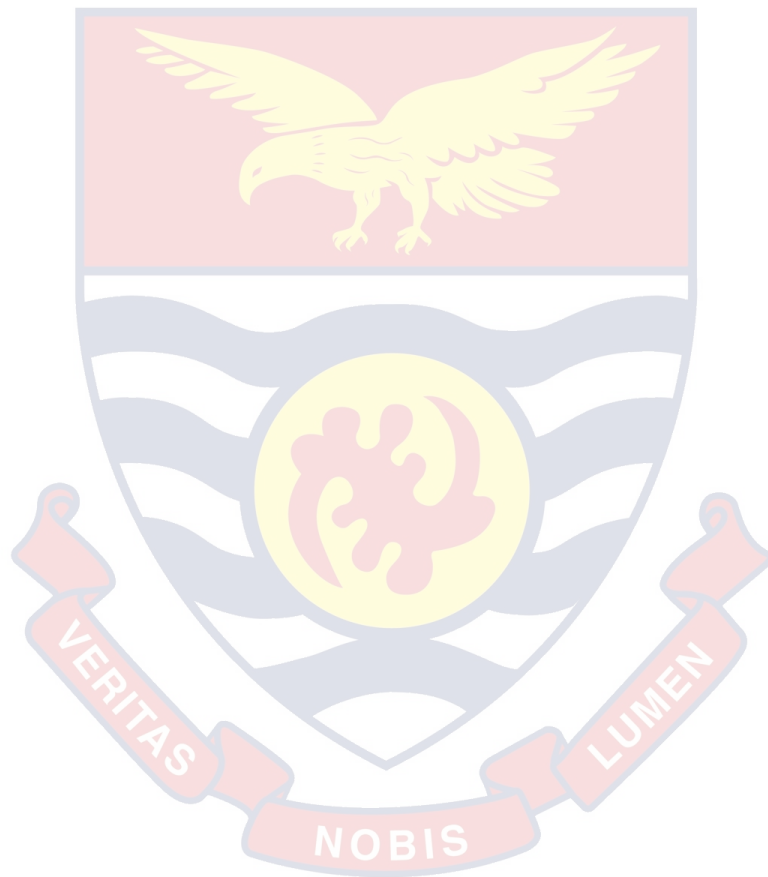


LIST OF ABBREVIATIONS

AAS	Atomic Absorption Spectroscopy
ADC	Analogue-to-Digital Converter
API	American Petroleum Institute
ASTM	American Society for Testing and Materials
BSS	Basic Safety Standards
CCD	Charge-Coupled Device
CPT	Cone Penetrometer
CW	Continuous Wave
EDXRF	Energy Dispersive X-ray Fluorescence
EPA	Environmental Protection Agency
FPSO	Floating Production Storage and Offloading
FS	Fluorescence Spectroscopy
FTIR	Fourier Transform Infrared Spectroscopy
FWHM	Full Width at Half Maximum
GAEC	Ghana Atomic Energy Commission
GC	Gas Chromatography
GNPC	Ghana National Petroleum Corporation
HCA	Hierarchical Clustering Analysis
HPGe	High Purity Germanium
HPLC	High-Performance Liquid Chromatography
IAEA	International Atomic Energy Agency
ICP-OES	Inductively Coupled Plasma Optical Emission Spectroscopy
INAA	Instrumental Neutron Activation Energy
LDA	Linear Discriminant Analysis

LIF	Laser-Induced Fluorescence
MATLAB	MATrix LABoratory
MCA	Multichannel Analyzer
NDT	Non-Destructive Test
Nd: YAG	Neodymium- doped Yttrium Aluminum Garnet
NMR	Nuclear Magnetic Resonance
NNRI	National Nuclear Research Institute
NORMs	Naturally Occurring Radioactive Materials
PARAFAC	Parallel Factor Analysis
PCA	Principal Component Analysis
PCC	Principal Component Coefficient
PC	Principal Component
PC1	First Principal Component
PC2	Second Principal Component
PCFV	Partnership for Clean Fuels and Vehicles
ROI	Region of Interest
ROST	Rapid Optical Screening Tool
RS	Raman Spectroscopy
SSD	Solid State Drive
SG	Specific Gravity
SOPCL	Saltpond Offshore Production Company
TEN	Tweneboa Enyenra Ntomme
TFA	Temporal Fluorescence Alteration
TRLIF	Time-Resolved Laser-Induced Fluorescence
UNEP	United Nations Environment Program

USGS	United States Geological Society
UV	Ultra Violet
Vis	Visible
WL	Working Level
XRF	X-ray Fluorescence



LIST OF SYMBOLS

S	Sulphur
N	Nitrogen
O	Oxygen
Si	Silicon
Li	Lithium
Na	Sodium
Cl	Chlorine
F	Fluorine
⁴⁰ K	Potassium-40
²²⁶ Ra	Radium-226
²³² Th	Thorium-232
⁶⁰ Co	Cobalt-60
<i>n</i>	Refractive index
$\bar{\nu}$	Antineutrino
e^-	Electron
Q	Quantum yield of fluorescence emission
Γ	The radiative decay rate of a fluorophore
λ	Wavelength
<i>I</i>	Fluorescence Intensity
A	Activity Concentration

CHAPTER ONE

INTRODUCTION

Background to the study

Crude oil, a complex, viscous organic fluid termed *black gold* is an indispensable commodity for the economic development of any country. It is the primary energy source for present civilisation, which nowadays accounts for 85% of global energy demand, and the tendency is forecasted to continue (Pedersen, 2011). Crude oil formation takes millions of years before its extraction. These natural oils are found in different parts of the world. They can be obtained from an extensive range of other geological sources and contain complex trace elements that characterise its geological composition and therefore, the oil field (Evdokimov & Losev, 2007).

Composites of crude oils include aliphatic, aromatic, high molecular weight organic compounds, non-hydrocarbon constituents containing Sulphur (S), Nitrogen (N), Oxygen (O), trace elements and salts (Hook, 2009). Trace elements such as Sodium, Magnesium, Iron, Cobalt, Vanadium and Nickel describe the properties of the host sediment and crude oil (Tamrakar, 2000). Their characteristics determine the type of technology to be used for drilling and refining. Due to different geological sources of the crude oils, its composition may vary from oil wells as well as from various oil fields (Appenteng et al., 2012; Asiamah, Asamoah, Mfodwo & Dasoveanu, 2013).

Getting to know the characteristics of the crude oil from a particular geological source is one of the critical determinants for optimisation during drilling. Besides, the features provide factual information about the kind of refinery technology needed for processing and environmental safety needs

(Tamrakar & Pitre, 2001). A tremendous amount of time, financial loss and environmental degradation would be incurred without proper data analysis to determine the appropriate technology to target the best drill site (Tamrakar & Pitre, 2001). Therefore, developing scientific practices and procedures for finding the characteristics of various crude petroleum oils from different geological sources is of much importance to the petroleum industry.

Studies have shown that chemical methods such as the Grote-Krekeler's method, Herman's method, Mortiz's method and other non-spectroscopic methods are used to determine the quality of crude oil. They require several hours of heating the samples to temperatures as high as 750 °C to obtain results (Adipah, 2019). These methods are not only destructive to the samples but also involve more than one process making it tedious and relatively expensive.

The simplicity of dealing and handling samples in spectroscopy has aided the development of new spectroscopic techniques to determine the physicochemical properties of petroleum products. These techniques have a unique diagnostic procedure and therefore gained relevance in crude oil analysis (El-Hussein & Marzouk, 2015). The most widely used non-destructive spectroscopic techniques in petroleum technology for crude oil analysis include Laser-Induced Fluorescence (LIF), X-ray Fluorescence (XRF) and Gamma Spectroscopy (GS) (Appenteng et al., 2012). The reason is that they offer rapid responses, high sensitivity and selectivity, and offer valuable information related to the intrinsic chemical characteristics of each examined sample (Appenteng et al., 2012).

Laser-Induced Fluorescence, X-ray Fluorescence and Gamma spectroscopic techniques have become the most preferred method used by

scientists for determining major and minor elements and minerals and provide higher precision and accuracy. Sample preparation is non-destructive, and spectral line interference is relatively uncommon. Specimen form can be solid, powder, gas, liquid or paste. Laser-Induced Fluorescence gives the fluorescence spectra profile of the light and heavy oils, which can be used to develop a standard wavelength fingerprint for crude oils (El-Hussein & Marzouk, 2015).

X-ray Fluorescence can be used to detect the elemental composition of substances. The simplicity of sample handling makes it advantageous over methods such as Instrumental Neutron Activation Analysis (INAA), which was used in the characterisation of the Jubilee and Saltpond crude oils (Appenteng et al., 2013). Though INAA was able to measure the sulphur concentrations, there was the problem of sample preparation using standards. This approach is relatively expensive and tedious as compared to X-ray Fluorescence spectroscopy, which uses computational tools to accurately determine the sulphur components in crude oil. High Sulphur containing natural oils generate hazardous levels of Sulphur dioxide (SO_2) with negative environmental and human health effects. Sulphur dioxide has respiratory consequences such as lung irritation, increased breathing rates and suffocation (Appenteng et al., 2013). The most devastating health effect is the aggravation of asthma, chronic bronchitis and irritation of the throat and eyes. It contributes to the formation of acid rain, which causes extensive damage to materials and terrestrial ecosystems, aquatic ecosystems and the human population (UNEP/PCFV, 2009).

Gamma spectrometry is a non-destructive and efficient method used in assessing potential health risks associated with exposure to naturally occurring

radioactive materials (NORMs) in crude oil. In Ghana, alpha and gamma spectrometry have been used to assess NORM scales generated from crude oil production in Ghana (Kpeglo et al., 2019). It is, therefore, feasible to use this technique to assess the radiological risks involved from exposure to crude oils from oil fields in Ghana.

With the commercial discovery of crude oil in the Jubilee Field of Ghana in June 2007, the purported speculations about the abundance of fossil and hydrocarbon reserves along the Gulf of Guinea (Coast of West Africa) was without a doubt a delightful dream come true (GNPC, 2009). Job creation and revenue generation, as a result, has augmented the national economy and invited more foreign investors to the country. There are only three oil fields in Ghana that are already producing (*Jubilee Oil field, Saltpond Oil Field and Tweneboah Enyenra Ntomme Oil Field*) out of 21 licensed blocks. Eight of these blocks were discovered over the last five years while companies such as Exxon, Anadarko, and Tullow Oil have established their presence in Ghana (Asiamah et al., 2013).

Research Problem Statement

Crude oil analysis is essential for characterisation and standardisation in the petroleum industry. This analysis calls for efficient techniques to obtain accurate information on natural oils. Currently, there is no information on the use of Laser-Induced Fluorescence, X-ray Fluorescence and Gamma spectroscopic techniques on the characterisation of crude oils from oils fields in Ghana. There has been no systematic analysis of these natural oils using these

spectroscopic techniques. Therefore, there is the need to use these non-destructive techniques to study these crude oils from oil fields in Ghana.

Research Questions:

Using Laser-Induced Fluorescence, X-ray Fluorescence spectroscopy, and Gamma Spectroscopy, is it possible:

- To systematically analyse and characterise crude oils from the various oil wells in Ghana and use this analysis to identify and classify them?
- To determine the quality of crude oils from the various oil wells in Ghana?

Research Objectives

The main objective of this research work is to use Laser-Induced Fluorescence, Energy Dispersive X-ray Fluorescence and Gamma spectroscopic techniques to characterise and determine the quality of crude oils from some oil wells in the Jubilee, TEN and Saltpond oil fields.

Specifically, the research will:

- i. Use Multivariate analysis methods to link the spectral signatures of the crude oils to their properties to identify and classify them.
- ii. Determine the Sulphur concentration in the various crude oil samples for comparative studies

- iii. Determine the activity concentration of naturally occurring radioactive materials (NORMs) in the crude oil samples for environmental pollution assessment.

The Rationale behind this Study

This proposed research aspires to explore the use of Laser-Induced Fluorescence (LIF), X-ray Fluorescence (XRF) and Gamma Spectroscopy (GS) for the characterisation of crude oils from oil fields in Ghana due to their advantage over other methods. The findings, using these techniques, will be used to confirm the superiority of this technique over others.

Delimitation

Crude oil samples for this work were obtained from the three main oil fields in Ghana (Jubilee, TEN, and Saltpond). Crude oil samples were obtained from the Floating Production, Storage and Offloading (FPSO) vessels FPSO KWAME NKRUMAH (Jubilee Field), FPSO MV25 (TEN Field) and SALTPOND WELLS 2 AND 4. The equipment used were available at the Laser and Fibre Optics Centre (LAFOC), Physics Department, University of Cape Coast and the National Nuclear Research Institute (NNRI) at Ghana Atomic Energy Commission (GAEC), Kwabenya.

Limitation

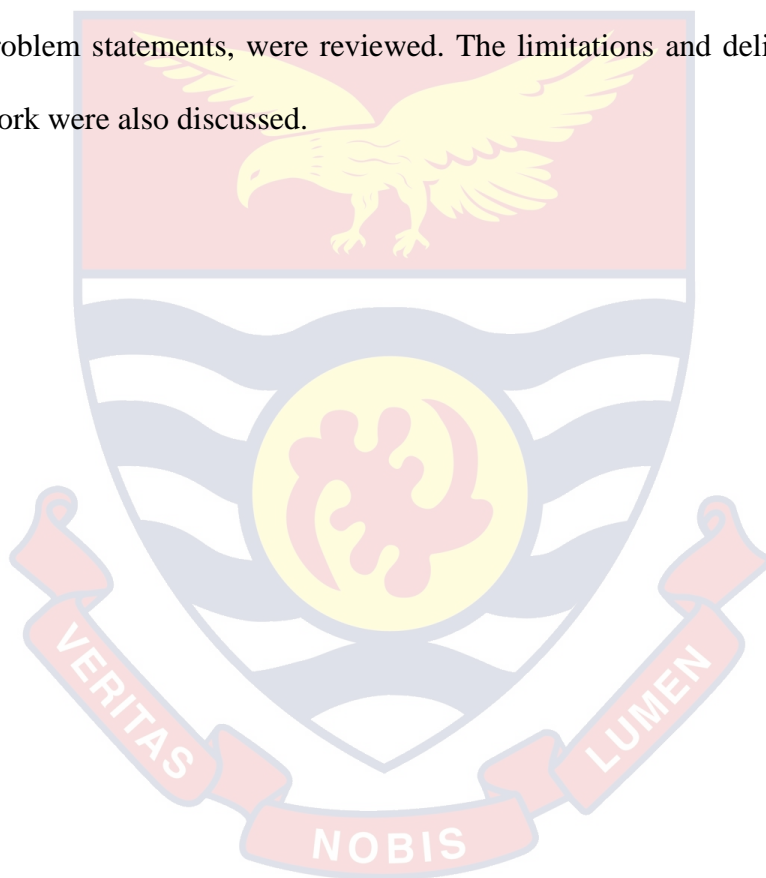
This study is limited to the determination of physicochemical parameters such as API gravity, specific gravity, naphthene and asphaltene content. This is due to the high cost involved. Oil samples from Sankofa Gye Nyame was omitted because this sector mainly produces natural gas.

The Organisation of the Study

Chapter 1 introduces and expounds the significance of this study and states the problems that this study seeks to address. Chapter 2 includes the study of the fundamentals of LIF, XRF and GS, the theoretical background of this work and a review of related previous studies. Laboratory methods for determining petroleum quality were also discussed. This chapter also discusses the composition of petroleum (Crude Oil) and radiation safety considerations in X-ray Fluorescence applications. Chapter 3 describes the methodology adopted for the experimental set-up, sample collection and preparation of various petroleum products and some crude oil samples from three oil fields in Ghana. The instrument used, its calibration and detector were also considered. Chapter 4 focuses on the result of the study, and chapter 5 contains a summary of the main findings of the research and discusses some economic potentials and recommendations.

Chapter Summary

This chapter expounded the background to the study which highlighted the socio-economic significance of crude oil, its composition, and how spectroscopic techniques such as Laser-Induced Fluorescence, Energy-Dispersive X-Ray Fluorescence and Gamma-Ray Spectroscopy can be used to effectively enhance crude oil analysis. The recommended methods by the researchers in differentiating between crude oil samples, which gave rise to the problem statements, were reviewed. The limitations and delimitations of this work were also discussed.



CHAPTER TWO

LITERATURE REVIEW

Introduction

The fundamental study of interactions of radiation with matter has become an enthralling developing research area in the petroleum industry. A thorough understanding of the Sulphur (S) content using fluorescence techniques can, therefore, not be underestimated (Martinez et al., 2004).

The latter-day discovery of crude oil across several regions in Ghana has awoken a growing attentiveness to research in the petroleum industry. Hence, a research work to determine the concentration of elements in crude oil from various oil wells in Ghana for quality assessment and standardization of petroleum products in Ghana.

Crude Oil Formation

When animals and microorganisms die and settle at the bottom of the earth over a very long period, several layers of mud cover them. With changes in heat and pressure over a long period, these layers are converted to kerogens which are estimated to be about 10^{16} tons of carbon. It is the most abundant content of living matter by 10,000 fold (Evdokimov & Losev, 2007). Due to heat and pressure, the kerogens are cracked to form crude oil which then migrates from one layer to another till it is trapped by a cap rock which is neither porous nor permeable, hence called the source rock (Ante, 2013).

Crude oil is made up of mainly organic carbon (85 – 87 %) and hydrogen compounds (12 – 14 %) with different complex mixes such as naphthenes, methane, butane, paraffin and other aromatic hydrocarbons (Evdokimov &

Losev, 2007). Petroleum is categorized as a naphthenic base, intermediate base or paraffin base depending on its hydrogen predominance. Tables 1 and 2 respectively spell out detailed information about the hydrocarbon and non-hydrocarbon composition of petroleum.

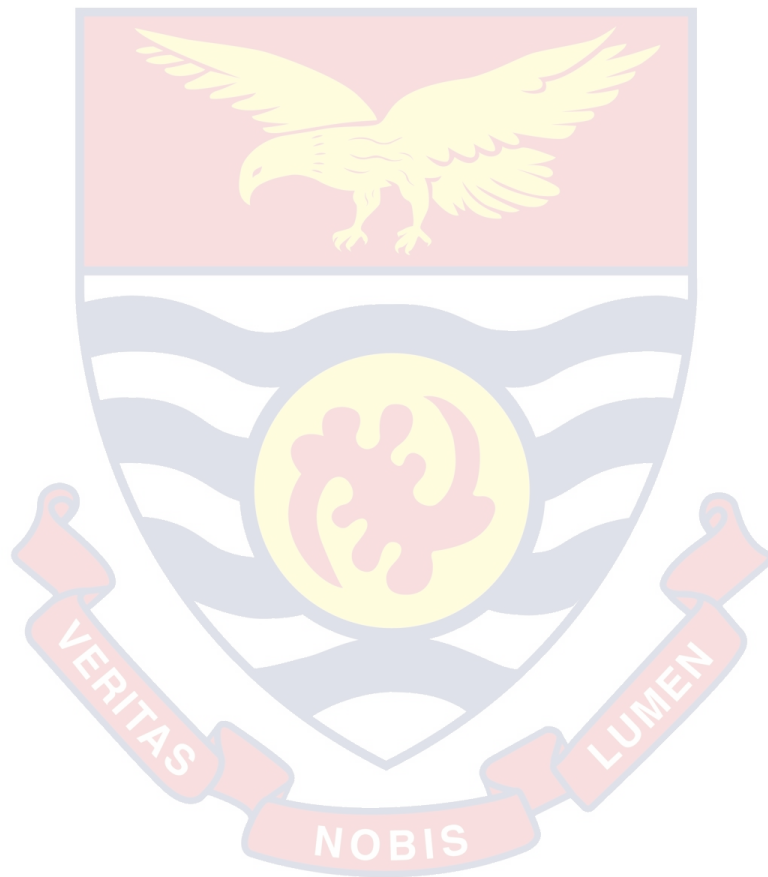


Table 1: Petroleum Hydrocarbon Composition (Hook, 2009)

Hydrogen family	Characteristics	Major hydrocarbons	Observations
Paraffin	Straight carbon chain	Methane, ethane, propane, butane, pentane, hexane	General formula C_nH_{2n+2} The boiling point increases as the number of carbon atoms increases. With the number of carbon atoms 25-40, paraffin becomes waxy.
Isoparaffins	Branched carbon chain	Isobutane, Isopentane, Neopentane, Isooctane	N/A
Olefins	One pair of atoms of a carbon	Ethylene, Propylene	General formula C_nH_{2n} In crude oil, olefins are not present but are produced during the process. Olefins with low molecular weight have excellent anti-knock properties.
Naphthenic compounds	5 or 6 atoms of carbon in the ring	Cyclopentane, Methylcyclopentane, Dimethylcyclopentane, Cyclohexane, 1,2-dimethylcyclohexane	General formula $C_nH_{2n+2} - 2R_n$ R_n is the number of naphthenic rings. By weight, the average crude oil contains around 50 % naphthene. Naphthenes are modestly good.
Aromatic compounds	6 carbon atom in the ring with three around the linkage	Benzene, Toluene, Xylene, Ethyl Benzene, Cumene, Naphthalene	In kerosene and lubricating oil, aromatic compounds are not desirable.

Non-Hydrocarbons

Table 2: Non-Hydrocarbon Composition of Petroleum (Hook, 2009)

Non-Hydrocarbons	Products	Observations
Compounds of Sulphur	Hydrogen Sulphide	Unwanted due to foul odour (0.5 % to 7%)
Compounds of Nitrogen	Quinoline Pyridine Pyrrole Indole	After exposure to sunlight, the presence of nitrogen compounds in gasoline and kerosene degrades the colour of the fuel. Gum formation can be caused by them. Less than 0.2 %, usually.
Compounds of Oxygen	Naphthenic acids, Phenols	At different stages of manufacturing, these acids cause corrosion and contamination issues. Traces of materials are up to about 2 %

Information on oil composition has increased based on recently developed apparatuses and techniques. Not only are scientists able to ascertain the group of hydrocarbon structure but also the whole make-up of the hydrocarbons and their respective structures (Hook, 2009). Examples of these new techniques include nuclear magnetic and paramagnetic resonances and X-ray fluorescence-based methods (Qasim, 2016). These techniques offer information about individual hydrocarbon composition. Contents of the trace elements in crude oil differ significantly, hence the upsurge in trace element studies by researchers across the global frontier (Hook, 2009).

The discovery and recovery of trace elements from crude oil are technically complex and has not been regularly used, although scientific

experimentation is in progress (UNEP/PCFV, 2009). Table 3 shows the elemental percentage range composition by weight.

Table 3: Elemental Percentage Range: (Bawazeer & Zilouchian, 1997)

Element	Composition (%)
Carbon	38 - 87
Hydrogen	10 - 14
Nitrogen	0.1 – 2
Oxygen	0.05 1.5
Sulphur	0.05 to 6
Metals	< 0.1

The physical and chemical properties of any given hydrocarbon species does not only depend on the number of carbon atoms present in the molecule but also on the nature and type of chemistry between them (Abdalla, 2015). The different proportions of the vast hydrocarbon class and distribution determine the yield and quality of refined petroleum products, without forgetting the percentage composition of single and other multi-elements and their influence on crude oil.

The market price evaluation of crude oil varies according to the prevailing standard price for all crude oil (Appenteng et al., 2013). The classification of crude oil into light and heavier grades is used to determine yield-quality since lighter grades produce quality yields whiles heavier grades have to undergo a process of carbon removal and hydrogen addition through catalytic cracking units (Abdalla, 2015).

Petroleum quality is linked to the concentration of Sulphur present . The API gravity of crude oil plays a major role in determining its worth on the world

market, with high gravity oils commanding higher prices. Globally, low sulphur content crude oils are rated as sweet. Sulphur concentrations differ around 0.1% to 0.5% for sweet and 1% to 3.3% for sour crude (UNEP/PCFV, 2009). Heavy grade and sour crude oils are more intricate to process, and as a result, relative to the light and sweet crude oils, they are uncommon on the market. In processing heavy oils, time, money and energy are consumed due to their low API-gravity (Hook, 2009) therefore making light and sweet crude oil the most valuable.

Oil Fields in Ghana

"Black gold" as crude oil is often referred to, is an essential commodity for the economic development of any country since it is a key factor for the socio-economic well-being of a country. In 2009, the World Energy Outlook issued a publication, which predicted a global demand in crude oil. Crude oil production was predicted to reach about 104 million barrels/day by 2020. The speculations about the abundance of fossil and hydrocarbon reserves along the Gulf of Guinea (Coast of West Africa), was, without doubt, a delightful dream come true, with the commercial discovery of crude oil Ghana (GNPC, 2009).

The recent discovery and commercialization of Ghana's crude oil is considered a blessing rather than a bane since the jobs that will be created and the revenue which will be generated will significantly improve the national economy. The discovery will also attract more foreign investors to the country. Thus, this economic commodity will enable Ghana join the growing economies globally and unlock the socio-economic benefits from its largely untapped oil wealth (Business Ghana, 2018). From a previous study (Abdalla, 2015), crude

oil production and commercialization in the regions of the Gulf of Guinea is estimated to have over 547 offshore oil and gas structures with the potential to meet the energy demands of the European Union and the United States of America.

Geographical Location of Crude Oil Sites in Ghana

Jubilee Field

The Jubilee Field is stationed in the Western Region in the South Atlantic Ocean of Ghana's coast. It is about 60 km offshore, between the Tano Basin and West Cape Three Points blocks. At 0 latitude, 0 longitude, and 0 altitude, it forms the southernmost tip of Ghana and the closest place to the sea. With a mean temperature of around 24.9 °C, it has a temperature range of 23.8 – 26.4 °C (Appenteng et al., 2012). Figure 1 is a map that shows oil wells, oil fields, basins and the different geological origins of crude oil in Ghana.



Figure 1: Map showing the different geological sources of crude oil that Ghana has

Saltpond Field

Saltpond oil field as shown in Figure 2 is an oil field off the coast of Ghana. The field was discovered in 1970 and currently operated by the saltpond offshore producing company (SOPCL). The oil field is 105 kilometres west of Accra, in a water depth of 80 feet (24 m). It stretches over an area of five square kilometres (1.95 sq miles) with geographical coordinates 5°12'0 north and 1°4'0' west. It has an average temperature of 24.7 °C (Appenteng et. al., 2013; Abdalla, 2015).



Figure 2: Saltpond offshore field showing the locations of two oil fields

TEN Field

After Jubilee Field, Ghana's second main oil field is the Tweneboa Enyenra Ntomme Oil Field. It is generally referred to as the TEN oil field, an acronym used in the three drilling fields that it contains as illustrated in Figure 3 (Abdalla, 2015). The Deepwater Tano block's equity partners are Tullow (44.95 percent), Kosmos Energy (18 percent), Anadarko (18 percent), Petro SA

(4.05 percent) and 15 percent of the Ghana National Petroleum Corporation (GNPC). The construction and assessment of the three deep wells began in 2013 following the approval of the licence in 2012 (Abdalla, 2015).

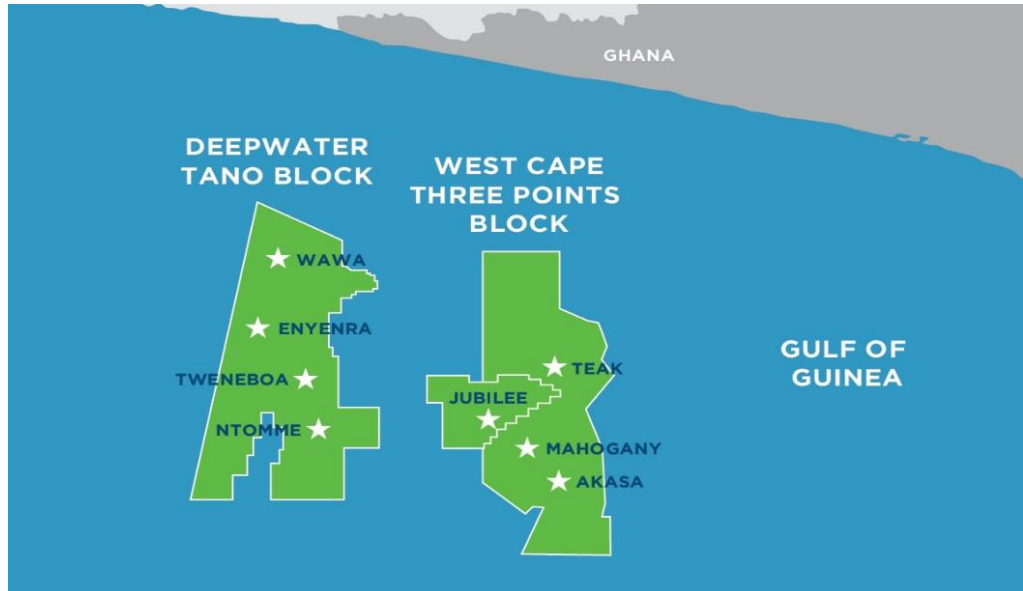
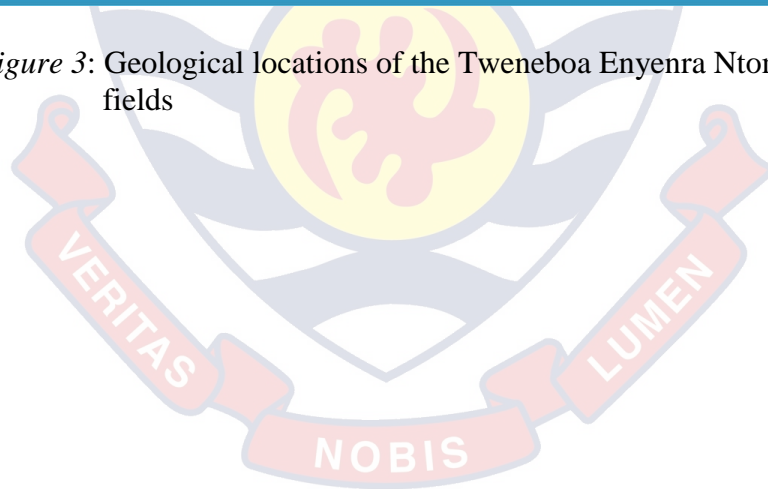


Figure 3: Geological locations of the Tweneboa Enyenra Ntomme (TEN) Oil fields



Laser-Induced Fluorescence (LIF) Spectroscopy

Description

Optical spectroscopic methods, which use radiations to study the effects of the source radiation and its interaction with the material, are often preferred (Svanberg, 2012) since several of the processes in the optical spectroscopy domain use non-ionizing radiation. They also require reduced space, low cost instrumentation and are simpler to set up (Frontasyova, 2011; Heftmann, 2004). In optical spectroscopy, reflection, absorption, transmission and scattering properties are studied to unearth the features of the materials such as its molecular composition, crystal structure, scattering coefficient and absorption coefficient. The techniques employed in optical spectroscopic experiments rely on information derived from the electronic transitional, vibrational and rotational energies of the molecules (Hollas, 2004; Svanberg, 2012). There are two analytical techniques used in determining the aforementioned parameters. These are elemental or atomic spectroscopy and molecular spectroscopy. Fluorescence Spectroscopy (FS), Absorption Spectroscopy, Fourier Transform Infrared Spectroscopy and Raman Spectroscopy (RS) represent some of the common measurement techniques used in molecular spectroscopy.

Fluorescence Spectroscopy is an optical technique in which emissions due to the absorption of photons into an atom is analysed (Sauer, Hofkens, & Enderlein, 2012). Fluorescence emission is caused by the electronic transitions of atoms and occurs within the optical range of the electromagnetic spectrum (300 nm – 700 nm). This technique is suitable for analysing molecules because of its sensitivity and specificity (Lakowicz, 2013; Svanberg, 2012). Solids and liquids exhibit broad fluorescence emission bands. Excited species usually in

the order of a few nanoseconds to microseconds de-excite after absorbing energy and emit light at a wavelength longer than the excitation wavelength. This fluorescent light is recorded with Photomultiplier Tube (PMT) or filtered photodiodes (Lakowicz, 2006).

The Fluorescence Process

The emission of light from any substance is called Luminescence and it occurs from electronically excited states. Luminescence is formally categorized into two groups, fluorescence and phosphorescence depending on the nature of the excited state (Lakowicz, 1998). Fluorescence occurs when the energy absorbed by a substance is released in the form of light, as the stimulating radiation continues (Pavia et al., 2008). The electron in the excited orbital, in the excited singlet state, is paired to the second electron in the ground-state orbital and the emission of photons rapidly allow the electrons to the ground state which is spin-allowed (Lakowicz, 1998). The emission rates of fluorescence are typically 10^8 s^{-1} so that a typical fluorescence lifetime is near 10 ns ($10 \times 10^{-9} \text{ s}$) (Lakowicz, 1998; Svanberg, 2004).

Theory of Fluorescence Emission

According to Lakowicz (1998), the most important characteristics of a fluorophore (fluorescent substance) are the fluorescence lifetime and quantum yield. The quantum yield is the number of emitted photons relative to the number of absorbed photons and the lifetime determines the time available for the fluorophore to interact or diffuse in its environment. The fraction of

fluorophores which decay through emission, and hence the quantum yield is given by

$$Q = \frac{\Gamma}{\Gamma + k_{nr}} \quad (1)$$

where (Γ) is the emission rate of the fluorophore and its nonradiative decay $S_0(k_{nr})$ (Lakowicz, 1998).

The fluorescence lifetime is near 10 ns. The expression for the lifetime is given by

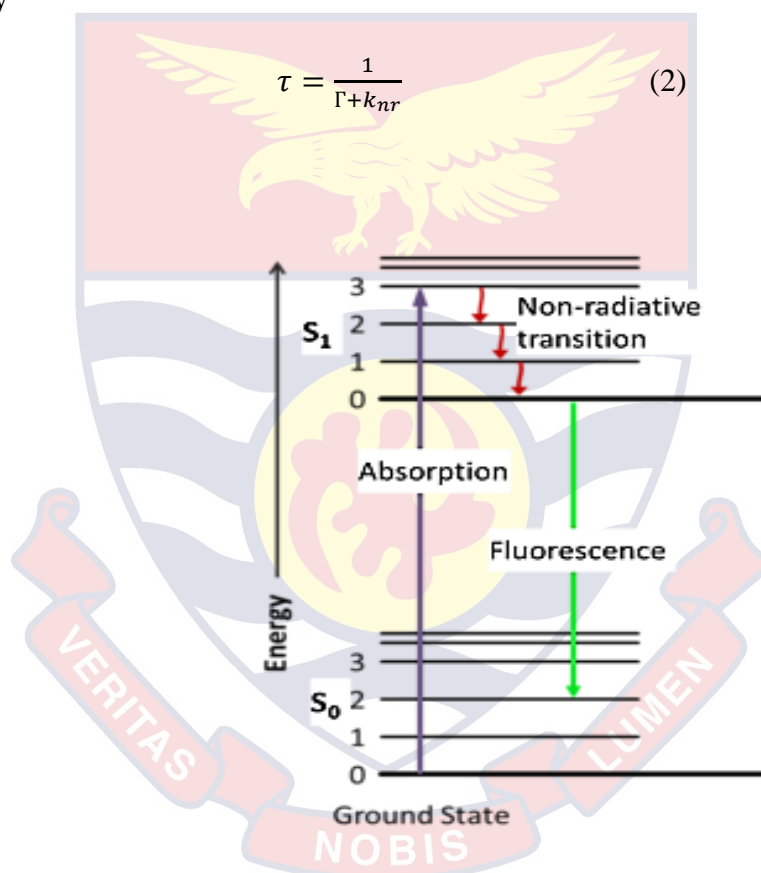


Figure 4: A simplified Jablonski diagram describing the fluorescence process

Figure 4 shows a simplified Jablonski diagram illustrating the fluorescence process and since few molecules emit their photons at precisely $t = \tau$, the lifetime is an average value of the time spent in the excited state. The lifetime of the fluorophore in the absence of a non-radiative process is called intrinsic or a natural lifetime and is given by

$$\tau_n = \frac{1}{\Gamma} \quad (3)$$

where τ_n is the natural lifetime.

The radiative decay Γ can be calculated using

$$\Gamma = 2.88 \times 10^{-9} n^2 \frac{\int F(\bar{\nu}) d\bar{\nu}}{\int F(\bar{\nu}) d\bar{\nu}/\bar{\nu}^3} \int \frac{\varepsilon(\bar{\nu})}{\bar{\nu}} d\bar{\nu}$$

$$= 2.88 \times 10^{-9} n^2 \langle \bar{\nu}^{-3} \rangle^{-1} \int \frac{\varepsilon(\bar{\nu}) d\bar{\nu}}{\bar{\nu}} \quad (4)$$

where $F(\bar{\nu})$ is the emission spectrum plotted on the wavenumber (cm^{-1}) scale, $\varepsilon(\bar{\nu})$ is the absorption spectrum, and n is the refractive index of the medium (Lakowicz, 1998). The integrals are calculated over the $S_0 \leftrightarrow S_1$ absorption and emission spectra and it works rather well, particularly for polynuclear aromatic hydrocarbons.

Data Pre-processing Techniques

Normalization, baseline correction, data noise reduction and resolution enhancement are some of the mathematical pre-processing techniques applied to spectroscopic data (Ozaki, McClure & Christy, 2006). These methods are employed in spectroscopy because fluorescence spectra suffer from drawbacks of undesired spectral variations as a result of light interaction with the samples, rigidity of the environment and noise from the detector (Amuah, 2020; Ozaki, McClure & Christy, 2006).

Normalization Methods

According to Ozaki (2006), normalization is a technique used in scaling samples to get all data on the same scale. Normalization methods include:

- 1) Maximum normalization: It involves dividing each observation by its maximum value instead of its average.

$$\bar{X}_i = \frac{X_i}{\max(X_i)} \quad (5)$$

- 2) Mean normalization: This type of normalization consists of dividing each observation of the data matrix by its average, thus eliminating the influence of any hidden factor.

$$\bar{X}_i = \frac{X_i}{\text{mean}(X_i)} \quad (6)$$

- 3) Unit normalization: This transformation normalizes sample-wise data X_i to unit vectors.

$$\bar{X}_i = \frac{X_i}{\sqrt{\sum_j X_{ij}}} \quad (7)$$

- 4) Area normalization: This transformation normalizes an observation (fluorescence spectrum) X_i by finding the area under the curve for the observation.

$$\bar{X}_i = \frac{X_i}{\sum_j X_{ij}} \quad (8)$$

Peak Deconvolution

Peak deconvolution can be described as the process of decomposing peaks that overlap with each other and extracting information about the hidden peaks depending on the existence of a baseline (Subhash & Mohanan, 1995; Smith, 2003).

Fluorescence is made up of bands representing the constituents of samples and these bands cover wavelength ranges. When the bands are broad they end up overlapping and close to each other (Lakowicz, 1998), hence the need to deconvolve the spectra (Subhash & Mohanan, 1995). After the desired spectrum has been acquired, the intensity and wavelength data of that spectrum is exported from the 001Base 32 software into a commercial software package MATLAB (MatLab R2019a) for further processing. At this stage, the entire spectrum is subjected to a processing procedure to obtain both the mean and normalized fluorescence spectra. The underlying algorithm for pre-processing is the Gaussian function fitting method, which was used in this work for deconvolving the fluorescence peaks contributing to the entire spectra.

The Gaussian Function Fitting Method for Fluorescence Spectra Deconvolution

The Gaussian distribution is commonly known as the “normal distribution” (Burke, 2019; Nave, 2020). Its probability density function is defined by Equation (9):

$$P(x) = \frac{e^{-\frac{(x-\mu)^2}{2\sigma^2}}}{\sigma\sqrt{2\pi}} \quad (9)$$

where μ is the mean, and σ^2 is the variance.

For peak identification, the mathematical procedure to fit experimental data with a Gaussian-like experimental function is described by Jean Jacqueline and Burke (Burke, 2019; Jacqueline, 2009). For a given data set of $(x_0, y_0), (x_1, y_1), \dots, (x_n, y_n)$, a direct fit with the function

$$y = ce^{\frac{(x-a)^2}{b}} \quad (10)$$

requires transformation into a new coordinate system as defined by Equations (11) and (12).

$$s_1 = 0, s_i = s_{i-1} + \frac{1}{2}(y_i - y_{i-1})(x_i - x_{i-1}), \quad (11)$$

$$t_1 = 0, t_i = t_{i-1} + \frac{1}{2}(x_i y_i + x_{i-1} y_{i-1}). \quad (12)$$

Coefficients a , b , and c in Equation 10 are obtained by solving equations 13 and 14

$$\begin{bmatrix} A \\ B \end{bmatrix} = \begin{bmatrix} \sum_{i=1}^n (s_i)^2 & \sum_{i=1}^n s_i t_i \\ \sum_{i=1}^n s_i t_i & \sum_{i=1}^n (t_i)^2 \end{bmatrix}^{-1} \begin{bmatrix} \sum_{i=1}^n (y_i - y_1) s_i \\ \sum_{i=1}^n (y_i - y_1) t_i \end{bmatrix} \quad (13)$$

The values of the coefficients are defined by Equation (14);

$$a = -\frac{2}{B}, b = -\frac{A}{B}, c = \frac{\sum_{i=1}^n y_i}{\sum_{i=1}^n e^{-\frac{(x-a)^2}{b}}} \quad (14)$$

where a , b , and c are the Gaussian coefficients used to generate the Gaussian peak approximations A and B in Equation 14

Implementation

The deconvolution procedure described in this chapter was implemented using Seasolve PeakFit Version 4.12 software package. Input data were data

points extracted from the Laser-induced fluorescence experiment collected on the 001Base 32 system in the form of Microsoft Excel files. The data structure used was a simple list of input points consisting of fluorescence wavelength and intensity parameters. Data output consisted of detected peaks, fitted standard errors, peak centroids, peak amplitudes, wavelength and intensity values of measured peaks and parameters of the approximated Gaussian function provided in the Microsoft Excel files.

Iterative Smoothing Method

Following the subsection of the entire spectrum to obtain both normalized and mean fluorescence plots of each sample from each oil field in this work, the extracted data for deconvolution was subjected to an iterative smoothing method. This is a Loess filter algorithm, which offers a non – parametric digital filter feature, which smoothens a set of data points based on some form of a sequential subset of points (Savitzky & Golay, 1964) until a suitable fit baseline, is obtained. After peaks were detected, each was fitted into a Gaussian function using the data set to calculate parameters that closely modelled the data set.

Principal Component Analysis (PCA)

Principal Component Analysis (PCA) is an exploratory and unsupervised pattern recognition statistical method used to divulge hidden structures within large data sets (Hotelling, 1933). It decreases the data set by plotting each fluorescence spectrum as a single point in PC space, based on the variations across the entire data set (McIntyre et al., 2020). It presents a visual illustration of the correlation between sample and variables and gives insight

into how measured variables cause samples to vary or show similarities among each other.

The Geometric Approach to Principal Component Analysis

A single sample of n observation vectors y_1, y_2, \dots, y_n forms a cloud of points in P dimensional space in Principal Component Analysis. Even though PCA can be applied to several distributions of y , it is significant to geometrically picture if the cloud of points is ellipsoidal (Jolliffe, 2002; Jackson, 1981). If the ellipsoidal cloud of points is not oriented parallel to either of the axes defined by y_1, y_2, \dots, y_n , the variables y_1, y_2, \dots, y_n in y are associated. Hence the need to establish the natural axes with the origin at the cloud of points. These new axes become the natural axes of the ellipsoid by translating the origin to \bar{y} and then rotating the axes. The axes are rotated with an orthogonal matrix B ($B'B = I$) multiplying each y_i .

$$z_i = By_i \quad (15)$$

The distance to the origin thus remains unchanged.

$$z_i^1 z_i = (By_i)' (By_i) = y_i^1 B' B y_i = y_i^1 y_i \quad (16)$$

The matrix adjusts y_i to a point z_i , which is the same distance from the origin as the rotated axis. The new principal components z_1, z_2, \dots, z_p in $z = By$ are uncorrelated, therefore making the $z, S_z = BSB'$ sample covariance matrix orthogonal, as expressed in equation 17.

$$S_z = BSB'_s = \begin{pmatrix} S_{z_1}^2 & 0 & \dots & 0 \\ 0 & S_{z_2}^2 & \dots & 0 \\ \vdots & \vdots & \ddots & \vdots \\ 0 & 0 & \dots & S_{z_p}^2 \end{pmatrix} \quad (17)$$

The sample covariance matrix is S .

From $D'SD = E = \text{diag}(\phi_1, \phi_2, \dots, \phi_n)$, where the ϕ_i 's are eigenvalues of S and D .

The orthogonal matrix B is also the transposer of the matrix D :

$$B = D' = \begin{pmatrix} a_1' \\ a_2' \\ \vdots \\ a_p' \end{pmatrix} \quad (18)$$

where a_i is the i th normalized eigenvector of S .

The principal components are the transformed variables and the diagonal elements of BSB' is on the right-hand side of Equation 18 are the eigenvalues of S . The eigenvalues of S are therefore the sample variances of the main components of the sample (Amuah, 2020; Jolliffe, 2011; Jolliffe, 2002; Jolliffe, 1986).

Hierarchical Clustering Analysis (HCA)

Hierarchical Clustering Analysis (HCA) is another unsupervised pattern recognition technique that identifies groups or clusters of data as a result of measuring the proximity between the elements. Groups of data can be defined based on similarity and dissimilarity.

Linear Discriminant Analysis (LDA)

Linear Discriminant Analysis (LDA) can be used as an easy means to identify the crude oil samples and also determine their geological location. It is laborious to determine the location of samples just by observing their fluorescence spectra (Amuah et al., 2017). Thus, the use of an identification and classification model (LDA) to identify the crude oil samples from the various oil fields used in this work.

LIF Measurement Techniques Used in Petroleum Research

Fluorescence spectroscopy has evolved in several forms for diverse applications. These include Laser-induced Fluorescence (LIF), Temporal Fluorescence Alteration (TFA) analysis, Rapid Optical Screening Tool (ROST), Time-Resolved Laser-induced Fluorescence (TRLIF), and Fourier Transform Infrared Spectrometry (FTIR) among several other techniques.

Apart from the sensitivity and good selectivity, LIF is without a doubt a significant tool for environmental monitoring (Baumann, Haaszio & Niessner, 2000; Balshaw-Biddle, 2000). The pollution of water and soil imposes a major threat to the environment and thus the need to use simple techniques to conduct thorough research without necessarily incurring cost (Schultze, Lemle, & Löhmannsröben, 2004). The use of LIF to study and analyse crude oil has enormous advantages compared to non-spectroscopic methods in terms of sample size, the precision of analysis, simplicity of sample handling and possible in situ measurements (El-Hussein & Marzouk, 2015). Fluorescence emission from crude oil is the result of the interaction between the aromatic compounds and electromagnetic radiation. The fluorescence spectra and their intensities are affected by the physicochemical properties of the samples under investigation (Löhmannsröben, Roch & Schultze, 1999; El-Hussein & Marzouk, 2015). It is therefore plausible to make use of LIF as a fast and straightforward spectrochemical tool in characterizing crude oil and petroleum-related products.

Temporal fluorescence alteration (TFA) analysis is the most common measurement technique used by organic petrographers as a characterization tool for sedimentary organic matter (Praider et al., 1990). This phenomenon occurs

under constant Ultraviolet (UV) irradiation of fluorescent macerals and largely involves irreversible and often spectacular changes in both colour and intensity. TFA analysis has been studied and used to understand the petrochemical basis of petroleum samples. Because of these observations studied in TFA analysis, organic petrographers now know that kinetics and amplitude of this phenomenon essentially depend on both maturity and type of the irradiated maceral (Praider et al., 1990).

The Rapid Optical Screening Tool (ROST) provides real-time field screening of the physical characteristics of soil and chemical characteristics of petroleum contamination at toxic waste sites (Bujewski & Rutherford, 1997). The ROST consists of a cone penetrometer probe (CPT) connected to a laser-induced fluorescence sensor. The ROST system can be deployed with any conventional CPT system containing a sapphire window that is mounted with the outside of the stainless-steel probe above the cone penetrometer tip (Fugro Geosciences Inc.). Light from an excited laser passes through the sapphire tip and information on the aromatic contaminants in the soil are fluoresced, thus making the ROST sensor a reliable field screening tool (EPA Research & Development, 1997).

Time-Resolved Laser-induced Fluorescence (TRLIF) spectroscopy is among several other powerful optical techniques used in petroleum research and exploration. TRLIF is a unique technique for fluorescent metal ion detection in petroleum products, soil and contaminated seawater samples (Takumi et al., 2012). TRLIF combined with parallel factor analysis (PARAFAC), demonstrated its unique applicability in the determination of uranyl (UO_2^{2+}) in the presence of silicic acid ($Si(OH)_4$) (Collins et al., 2011) an also a useful

method to detect oil contamination in water up to a concentration of 0.5 ppm (Schade et al., 1992). Finding the concentrations of elements in crude oil samples could prove futile especially when the technique in question does not provide information on the concentration levels in the oils (Takumi et al., 2012).

Inner Electron Spectroscopy

X-rays are highly energetic electromagnetic waves which are produced whenever fast-moving electrons are brought to rest. The radiation produced consists of the *Bremsstrahlung* and the characteristic part. The *Bremsstrahlung* (continuous part) is produced as a result of the deceleration and change in motion direction of the charged electrons when bombarded, thus exciting the atom to a higher energy level. The transition to a lower energy state occurs through an electron-hole that is observed to move out of the other shells as shown in Figure 5. A series of emission lines are obtained correspond to the successive atomic energy loses. The transition is denoted by K_{α} , K_{β} , K_{γ} etc corresponding to the movement of the electron hole from the L- shell to the L, M shell. (Svanberg, 2012).

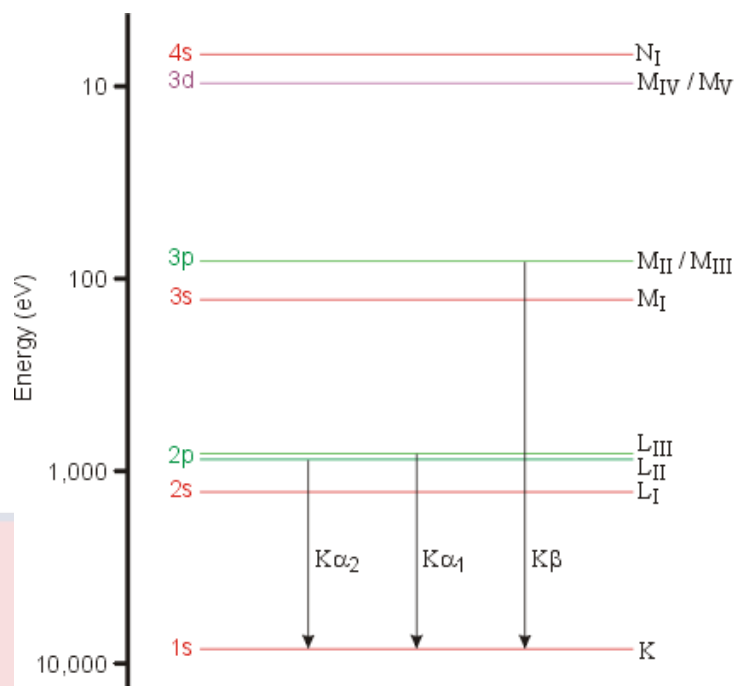


Figure 5: X-ray Transition of inner electron energy levels

Wilhelm C. Röntgen discovered X-rays and announced the existence of electromagnetic radiation with a wavelength comparable to the distance between crystal planes (~ 0.1 nm). M. Von Laue, William Henry Bragg and William Lawrence Bragg investigated this in their study of crystal structures utilizing X-rays. This was an important milestone in the development of X-ray crystallography. The wavelength of a large number of emission lines has now been very accurately ascertained and atomic X-ray investigations have resulted in a very precise charting of the energy levels for inner electrons (Svanberg, 2003). The chemical environment of the atoms has a comparatively lesser effect on the energy states of the inner electron shells. Hence, a spectral examination of the characteristic X-ray emission is well suited for elemental analysis. Moseley's law gives the relation between the wavelength of a particular X-ray line and the nuclear charge Z of the corresponding atom;

$$1/\sqrt{\lambda} = C(Z - \sigma) \quad (19)$$

The law states that *the square root of the frequency of emitted X-rays is proportional to the atomic number*. C and σ are constants characterizing a specific spectral species (Svanberg, 2003). The law of Moseley can be derived from the basic atomic model of Bohr. A Moseley diagram for K_{α} and L_{α} emission is shown in Figure 6. Using such an illustration, identification of elements is possible in a sample.

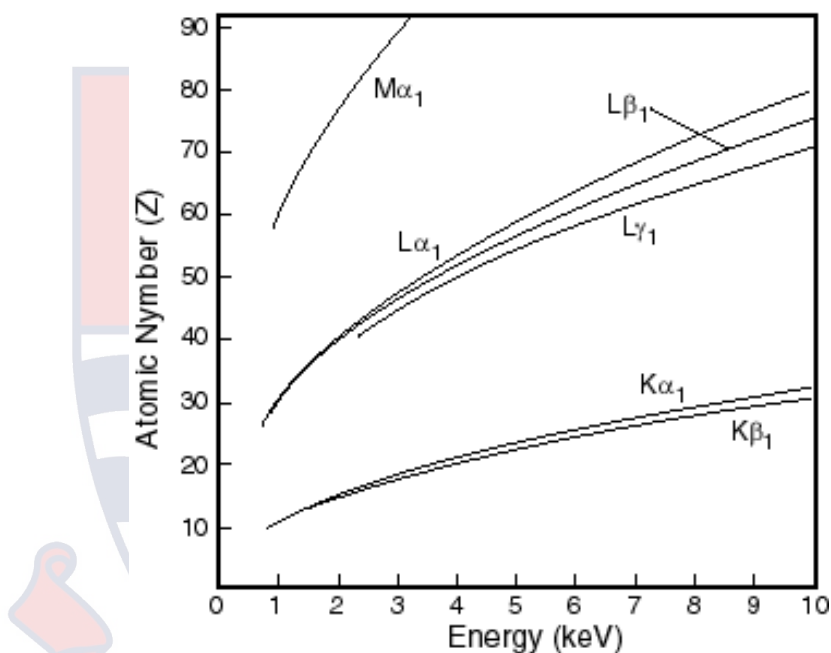


Figure 6: Diagram illustrating Moseley's Law

X-ray Emission Spectroscopy

X-ray emission, which can be induced in different ways (the use of energetic electrons and heavier charged particles), is one of the techniques of classical inner shell photoelectric effect. By irradiating the sample with X-ray radiation, it is likely to create an inner shell vacancy resulting in fluorescence observation. Fluorescence is a process in which a part of energy absorbed by a substance is discharged in the form of light as long as the stimulating radiation continues (Hercules & Joyner, 1979).

Energy Dispersive Spectroscopy

X-ray processing using an energy-dispersive device is effective. No analysis of the crystal is required in this method, as the radiation falls directly onto an energy-dispersive detector. A silicon lithium-doped detector (Si (Li)) is used to produce voltage pulses proportional to the energy of the X-ray quanta. The pulses are sorted out according to their amplitude (energy) in a multi-channel analyser using an Analogue-to-Digital Converter (ADC) (Svanberg, 2003). The full spectrum gradually emerges on a system display with linewidth obtained from a 150 eV (Si -Li) detector. The energy-dispersive system allows for multi-element analysis (Svanberg, 2012).

The Sensitivity of the System and its Application in Petroleum Research

The sensitivity of a system is generally expressed as the ratio of the signal of a standard sample to the root mean square noise level. This allows comparisons to be made among diverse techniques and procedures used in experimental research across laboratories globally. The use of light and light-based techniques in spectroscopy to investigate sample characteristics and probe material properties have invariably become widespread among researchers in recent years (Wang, Cheng & Wang, 2005). Spectroscopic techniques often require minimal or no sample preparation and provide rapid analysis since they are non-destructive (Wang, Cheng & Wang, 2005; Demtröder, 2013).

The production of fuel has adapted to a worldwide trend, which is the decrease in harmful substances in combustion products (Daučík, 1998). In choosing the method for determination of elemental composition in crude oils

and petroleum fuels, there exist many possibilities of standardized procedures that are recommended or applicable to individual fuel grades, hence the need for an analysis method such as X-ray fluorescence. The assessment of Sulphur concentration in diesel oils, aviation fuels and crude oils by the Slovak Technical Standard, which is identical to the European Standard is followed by two prescribed methods: the determination of elemental composition by Wickbold's method and Grote-Krekeler's method (ASTM D 1551) proved to be uncomfortable.

The essence and interest in finding and measuring the concentration of element composition in crude are because almost all elements of the periodic table are found in crude petroleum oil (Steffens, Landulfo, Courrol & Guardani, 2011). Information on these elements is necessary and significant for oil field development, drilling and environmental pollution assessment (Appenteng et al., 2013). For the multi-element analysis of the Saltpond and Jubilee crude oil, Instrumental neutron activation analysis (INAA) was used (Appenteng et al., 2012). Significant progress was made in identifying 18 trace elements as shown in Figure 7.

INAA		
Trace metals	Trace element concentration ($\mu\text{g/g}$)	
	Saltpond crude oil	Jubilee crude oil
Al	2.71 ± 0.446	4.09 ± 0.633
As	0.681 ± 0.135	0.127 ± 0.072
Br	1.14 ± 0.069	1.61 ± 0.112
Ca	1.21 ± 0.15	8.47 ± 0.932
Cd	ND	ND
Cl	14.3 ± 1.289	66.9 ± 4.503
Co	(2.86)	(0.191)
Cu	0.293 ± 0.011	0.527 ± 0.172
Fe	5.88 ± 0.143	32.4 ± 2.29
K	0.785 ± 0.233	2.03 ± 0.814
Mg	1.15 ± 0.142	0.443 ± 0.014
Mn	0.048 ± 0.005	0.170 ± 0.012
Na	101 ± 5.06	324 ± 9.845
Ni	12.6 ± 0.927	3.22 ± 0.284
S%	$0.194 \pm 0.06\%$	$0.242 \pm 0.011\%$
Si	ND	ND
V	3.71 ± 0.631	2.41 ± 0.524
Zn	0.375 ± 0.029	0.585 ± 0.057

Data behind \pm are standard deviations

Figure 7: Results of Trace Elements found in Saltpond and Jubilee Oil

Although INAA has numerous merits among which include no sample processing, high precision, selectivity, and requiring minimal sample preparation, XRF analysis was found to be simpler and straightforward. By comparing the results obtained to other techniques such as Hermann's Method, Mortiz's Method and Grote-Krekeler's Method (El-Hussein & Marzouk, 2015) and it can be inferred that the EDXRF technique is fast, simple, and precise (Svanberg, 2003).

Application of X-ray Spectroscopy

- Petroleum Research
- Analysis of geological samples
- Metallurgy (e.g. quality control)
- Ceramic and glass manufacturing
- Cement production.
- Mining
- Soil surveys
- Research in igneous, sedimentary, and metamorphic petrology

Merits of X-ray Spectroscopy

- Used for determining the structure of a substance.
- It is the method of choice for elemental composition determination in which other parameters such as bond lengths and bond angles are often calculated if other spectroscopic techniques fail to disclose known compounds.

Demerits of X-ray Spectroscopy

- This approach is very tedious, time-consuming and requires a professional hand.

Naturally Occurring Radioactive Materials in Petroleum

Introduction

Studies on radioactive materials have shown that coming into contact with extreme levels of radiation can lead to damages to the human tissues. An epidemiological study concerning people exposed to radiation during the 1945 atomic bombing of Hiroshima and Nagasaki has proven that exposure to radiation has the potential to delay malignancies. Thus, it is significant to note that activities that involve exposure to radiation be subject to a strict safety standard to protect the human population exposed to radiation (IAEA, 1996).

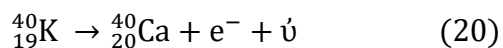
Information about the radioisotope signatures is key for radiological risk and hazard assessment since members of the public and personnel are mostly the ones exposed to contaminated petroleum substances (Kpeglo et al., 2019). Oil exploration and exploitation activities have started at different geological sites along the west coast of Ghana over the last decade. A documented problem in the production of oil in Ghana is the accumulation of scale on the inside faces of oil production pipes.

Scales are made up of barium sulphate, barium carbonate, and calcium carbonate. NORM scale is produced when Ra (radium) dissolved in the formation water is co-precipitated with Ba, Sr, or Ca as mostly sulphates. These materials form insoluble hard deposits within the manufacturing equipment (Smith et al., 1999) and depending on the formation and age of the well, scale management can lead to significant health and environmental hazards for both employees and the public if not treated properly (Kpeglo et al., 2019).

Environmental Concerns

Uranium, radium, thorium and radon are naturally occurring radionuclides dissolved in very minute concentrations during chemical reactions between water and rocks (Fisher, 1998). The coexistence of groundwater and petroleum oil reveals a significantly high concentration of dissolved mineral constituents that accumulate during prolonged periods of water or rock contact. Majority of waters located in oil fields are rich in chloride, and this enables the solubility of other elements including radioactive element radium, which is one of the more dangerous uranium decay products (Edward, 2016). It is a radioactive heavy metal and a potent alpha emitter. As it decays, it produces radon gas as a by-product. Radium is chemically similar to calcium, so when ingested, it migrates to the bones, the teeth and the milk (Edward, 2016; Garvin, 2011). While some radium is still used for medical purposes, only small quantities are needed. Most of the world's radium is discarded with the crushed rock left over from uranium mining, even though it is known to be a hazard (Edward, 2016). The radioactive decay of uranium and thorium found in rocks produces Radium-226 and Radium-228 (USGS, 1999).

Potassium-40 (^{40}K) is a radioactive isotope of potassium, which has a half-life of 1.251×10^9 years. It makes up 0.012 % (120 ppm) of the total amount of potassium found in nature. Potassium-40 decays to calcium-40 (^{40}Ca) with the emission of a beta particle (β^- , an electron) (Audi, Bersillon & Blachot, 2003) with a maximum energy of 1.31 MeV and an antineutrino as shown in Equation 20:



where $\bar{\nu}$ is an antineutrino and e^{-} is an electron.

There is no danger from the radiation coming from the ^{40}K that makes up 0.012 % of the total amount of potassium found in nature (Shawky et al., 2011).

Thorium, with atomic number 90, is a weakly radioactive metallic chemical element that decays very slowly through alpha decay (Audi, Bersillon & Blachot, 2003). Thorium, bismuth and uranium on Earth are the only three radioactive elements that still exist naturally as primordial elements in significant amounts. Thorium-232 (^{232}Th) is a health risk in the environment because of the rapid build-up of radium-228 (^{228}Ra) and its associated gamma radiation (Environmental Protection Agency, U.S.A, 1997; Kpeglo et al., 2019). Radon-220 (^{220}Rn) and its decay species cause lung infections. Thorium is present in very low quantities almost everywhere in the environment; Humans are exposed to it in air, food and water (Environmental Protection Agency, U.S.A, 1997).

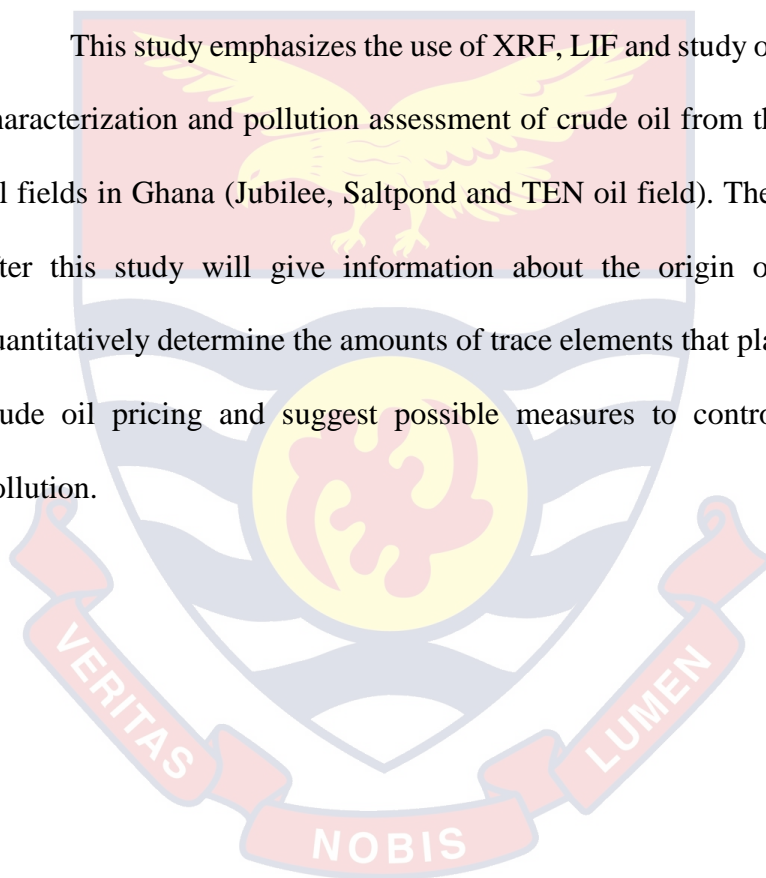
Significance of Assessing NORM Presence in Crude Oil in Ghana

The evaluation of scale and sludge handling resulting from the production of crude oil in Ghana indicates potential future health risks for workers, the public and environment if they are not properly controlled (Kpeglo et al., 2019). Radioactive characterization of NORM in crude oil production has not been investigated in crude oils from the main oil fields in Ghana (Jubilee, TEN, and Saltpond). There is the need to study, measure and assess the activity concentration of radionuclides such as Radium-226, Thorium-232 and Potassium-40 in Ghanaian crude oils for quality assessment.

Chapter Summary

Researchers in petroleum exploration and research have utilized the X-ray fluorescence and Laser-induced fluorescence techniques among several other relevant techniques already mentioned. In the absence of any other advanced techniques used to analyse and research crude oils and petroleum products, it is possible to fall back on simple and straightforward spectrochemical techniques.

This study emphasizes the use of XRF, LIF and study of NORMs for the characterization and pollution assessment of crude oil from the three (3) main oil fields in Ghana (Jubilee, Saltpond and TEN oil field). The results obtained after this study will give information about the origin of the crude oil, quantitatively determine the amounts of trace elements that play a major role in crude oil pricing and suggest possible measures to control environmental pollution.



CHAPTER THREE

RESEARCH METHODS

Introduction

This chapter details the research process, thus provides information on the samples, measurements and analysis procedures used in this research. This chapter also explains the various stages of the research.

Samples

Four different composite run-down petroleum crude oil samples in bottles, as shown in Figure 8, were used for the study. They were obtained from the Jubilee, TEN, and Saltpond oil fields through the Research and Development Unit of Ghana National Petroleum Corporation (GNPC). The samples were transported from GNPC in polystyrene boxes and kept at room temperature for measurements to be taken. Table 4 shows a summary of the crude oil samples, oil field locations and sample codes used.



Figure 8: Crude Oil samples in bottles obtained from the Jubilee, TEN and Saltpond oil fields

Table 4: Summary of the Crude Oil samples, Oil Field Locations and sample Codes used

Crude Oil Sample	Oilfield/Drilling	Sample Code
FPSO Kwame Nkrumah	Jubilee	JF
FPSO MV25	Tweneboa Enyenra Ntomme	TF
Saltpond Well 2	Saltpond	SF 1
Saltpond Well 4	Saltpond	SF 2

The Oil Fields

Located between the Deepwater Tano and West Cape Three Points blocks, is the Jubilee field, and its location in the sea at $4.492^{\circ} N$ $2.916^{\circ} W$ is shown in Figure 9.

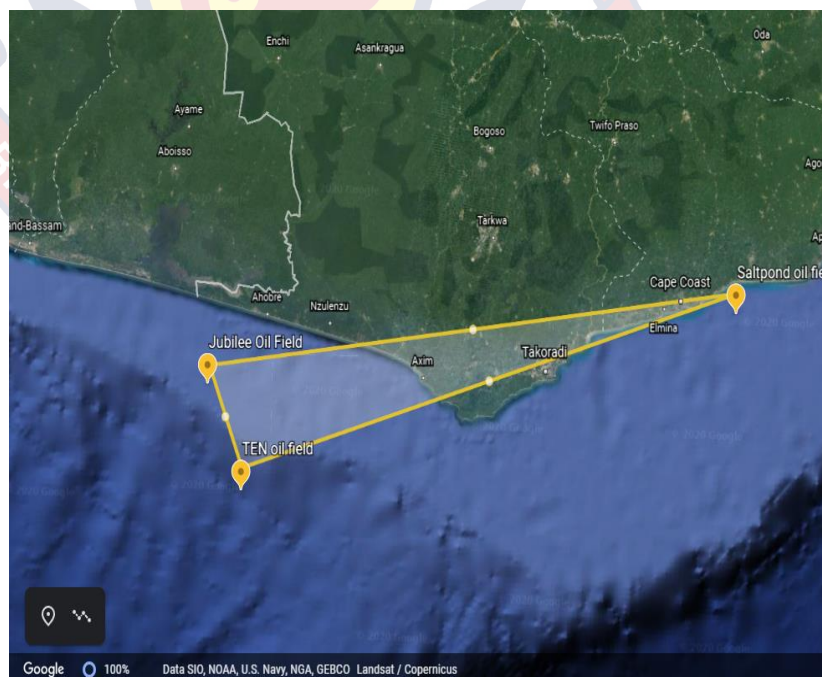


Figure 9: Satellite view showing the three oil fields with their geological positions along the Saltpond and Takoradi coastal arches

Figure 9 shows the sampling sites and geographical coordinates of the two other offshore oil fields, Tweneboa Enyenra Ntomme (TEN) and Saltpond respectively. The TEN oil field lies 19.3 kilometres west of Jubilee field at $4.49278^{\circ} N$ $2.916667^{\circ} W$ while the Saltpond oil field lies in the Takoradi Arch ($5.093^{\circ} N$ $1.069^{\circ} W$) approximately 220 kilometres from the Jubilee and TEN oil fields.

Laser-Induced Fluorescence (LIF) Measurement

Experimental Set-Up

This spectral research or analysis setup consists of a source of radiation, an analyte and a detection device. The radiation source is a continuous-wave (CW) diode laser with a 100 mW maximum output power emitting at a wavelength of 405 nm. It is equipped with a laser diode driver requiring an output voltage and current of 12 V and 2 A, respectively, with TTL modulation of 0 to 20 kHz. Optical components such as the bifurcated optical fibre probe (Ocean Optics, U.S.A) and a fibre port micro-positioner (PAF-SMA-5B, Thorlabs, U.S.A) were used. The bifurcated optical fibre with a core diameter of 600 μm was connected to the fibre port positioner, which directed the beam out of the microscope objective lens (CP09/M, Thorlabs, U.S.A). When in operation, the optical fibre cable acts as an entrance slit through which light enters.

The detection system, which is made up of a CCD-based USB2000 spectrometer (USB2000, Ocean Optics) and a 450 nm cut-off long pass filter, was employed to detect the fluorescence of the crude oil samples. It operates on low power characteristics of 100 mA at 5 V. Within the range of 200 nm to

1100 nm, this spectrometer is responsive to photon activity. The light is dispersed by an asymmetric cross Crenzy-Turner optical bench onto a 2048-element, linear silicon CCD array detector. Data from the CCD detector is acquired by choosing from 1 ms to 60 ms as integration time. The data collected is transformed into digital information and passed to the 001Base32 spectrometer operating software of the Ocean Optics USB2000 spectrometer on the PC for visualization.

The 001Base32 spectrometer operating software is a 32-bit user-customizable software for advanced retrieval and display program. It displays measurements in real-time, which allows the user to make selections and adjustments. The software is fully computer-controlled for data acquisition and a large number of data can be saved automatically and exported to other software platforms for further analysis.

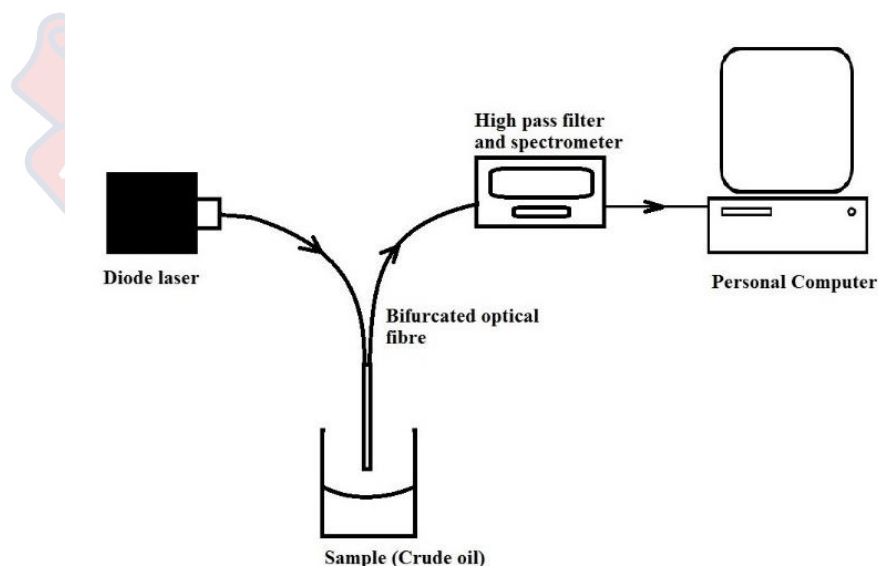


Figure 10: Schematic diagram for the LIF measurement set-up showing the radiation source (Diode Laser), the analyte (Crude Oil), optical components (Fibre Probe) and the detecting system (Spectrometer with Filter)

LIF Measurement

A laser source was used to measure the fluorescence intensities from the four (4) crude oil samples at the Laser and Fibre Optics Centre (LAFOC), Department of Physics, U.C.C. Five (5) replicates of each of the four samples were labelled: JF, TF, SF 1, and SF 2. A 405 nm CW diode laser was incident on each sample. The emitted fluorescence was harvested and transmitted through an optical fibre to a long pass filter, and then to the USB2000 spectrometer (Ocean Optics, U.S.A). The fibre was positioned behind a converging lens 90 degrees from the sample and the spectrum displayed on a computer screen. The data from each sample was saved after the spectrum was acquired. The intensity and wavelength data of that spectrum was exported from the 001Base32 software into MATLAB (Matlab R2019a) for further processing and analysis.

Data Analysis of LIF Measurement

The fluorescence spectra from each sample were deconvolved to extract information about the hidden peaks contributing to the entire spectra. Two unsupervised pattern recognition techniques, Principal Component Analysis (PCA) and Hierarchical Clustering Algorithm (HCA) were used to determine the similarities or differences in the samples used. The Score plot of the PCA was used as input variables to generate a classification model. These Principal Components (PC1 and PC2) were used to generate the Linear Discriminant Analysis model for the identification and classification of the samples.

Six hundred (600) LIF spectra were obtained from the four crude oil samples measured from the four different oil wells. Four hundred (400) LIF spectra representing 66.67% of the entire LIF spectra obtained were used for the

training set. The 200 LIF spectra representing 33.33 % of the total LIF spectra were used for the verification set.

X-ray Fluorescence Measurement (XRF)

Experimental Set-Up

In this study, the AMP TEK X-123 Experimenter Kit with a fast SDD detector (AMP TEK INC., U.S.A) was employed. This system includes a stainless steel 316 (SS316) test sample, a Mini-X USB controlled X-ray tube (radiation source) designed with a collimator and filter holder and an XRS-FP2 quantitative analysis software package interfaced with a computer for material analysis. It can be used in three different modes of application:

- Single-layer samples, for compositional and single-layer thickness analysis (XRS-FPS BULK)
- Multi-layer thin film samples, for compositional and multi-layer thickness analysis (XRS- FP2 MTF)
- Single-layer samples, for compositional and single-layer thickness using an incident electron beam instead of an X-ray beam (XPS-FP2 EPXA)

The radiation source and test stand with shielding and sample enclosure eliminate the risk of radiation leakage as shown in Figure 11 and Figure 12 respectively.



Figure 11: In-built Mini-X Radiation Source



Figure 12: AMPTEK EXP-1 X-123 XRF experimenter kit showing the radiation source (Mini-X-ray Tube) and spectrometer (X-123) both situated beneath the radiation shielding compartment

Scale Calibration in the Amptek DPP MCA

The scale calibration in the Amptek DPP MCA software is elaborated in the following steps:

- Two peaks were chosen for the calibration and their energies noted.
- The ROI around each peak was marked. By holding down the “U” key, the cursor highlighted the entire peak by clicking the left base of the first selected peak.
- The “Calibrate” toolbar key was used to access and move the calibration dialogue box to show the peaks. The peak was highlighted and information filled in.
- The beginning and endpoints of the regions of interest were adjusted and the Centroid button on the dialogue box clicked to enter the centre position of the peak into the Channel box. The energy of that peak was entered into the Value box and the “Add” button clicked.
- The cursor was again clicked into the second peak following similar steps used earlier for the first peak.
- The energy units keV were entered into the Unit box to finally calibrate the scale in keV.

XRF Measurement

With calibrated Pasteur tip ejector pipette, each of the samples was moved into 2 mL plastic cups held by transparent sheaths called Mylars. In order to prevent any surface contamination, the Mylars were soaked in concentrated acetone and washed with purified water. Four replicates of each

sample were analysed to verify the reliability of measurements in terms of precision and consistency.

The X-ray fluorescence measurements were taken at the National Nuclear Research Institute (NNRI) facility at GAEC, Kwabenya. Four sets of samples were sent to the Spectrometry laboratory and exposure to radiations conducted using the EXP-1 XRF Experimenter Kit. The setup was operated at a voltage of 45 kV and current 5 μ A. The system includes an X-123 complete spectrometer with an SDD detector and a DP5 Digital Signal Processor. The X-ray tube (Mini-X) has a collimator, a place to mount filters, provides a radiation-shielding compartment with safety interlocks and a sample chamber. Figure 13 shows the shielding compartment with its safety plunger, while Figure 14 shows the sample holder in the shielding compartment.



Figure 13: The shielding compartment with safety plunger showing the safety features of the AMPTEK EXP 1 X-123 XRF experimenter kit.



Figure 14: Sample holder in the shielding compartment of the AMPTEK EXP 1 X-123 XRF experimenter kit showing the sample-detector configuration

Data Analysis of XRF Measurement

Qualitative analysis to identify the elements present in the sample was carried out using the Amptek DPP MCA software package for spectrum analysis. With features such as background subtraction, centroids of known regions of interest, spectra scaling etc., trace element identification can be achieved with ease. The data obtained was saved in ASCII or Amptek MCA formats that most software will recognize. Quantitative analysis to obtain the sulphur concentrations of the crude oil samples measured was performed using the bAxil software version 1.6. The software was able to compute the elemental concentrations from the analysed spectra using computations based on the Fundamental Parameter method without making use of standards.

Gamma Ray Spectrometer Measurement

Experimental Set-Up

In this study, the AMETEK ORTEC High Purity Germanium (HPGe) GEM series coaxial detector system (P and N-type) at the National Nuclear Research Institute, GAEC, Kwabenya was used. Its resolution (Full Width at Half Maximum) at 1.33 MeV is 1.8 keV with a Peak-to-Compton ratio of 62:1 and a nominal efficiency at 1.33 MeV. It has a cryogenic cooling system, which uses both liquid nitrogen and an electro-mechanical cooler.

Multichannel Analyser

The DSPEC LF Digital Signal Processing gamma spectrometer in Figure 15 was used in analysing a stream of voltage pulses and sorting them out into a histogram or "spectrum" of several events versus pulse-height, which often relates to the energy or time of arrival. The DSPEC LF has an ADC conversion gains up to 64 K channels for expanded energy range applications. With a USB 2.0 Ethernet (TCP/IP) connectivity, Low-Frequency Rejector (LFR), large front panel display for at-a-glance system status information, a digital spectrum stabilizer and a "Loss Free" or "Zero Deadtime (ZDT)", the DSPEC LF supports all HPGe detector types, old and new.



Figure 15: DSPEC series multichannel analyser (AMETEK ORTEC, U.S.A)

Gamma Ray Measurement

For gamma-ray determinations, the samples were each transferred in 500 ml Marinelli beakers and sealed with masking tape to avoid spillage as shown in Figure 16. The samples were analysed by a High Purity Germanium (HPGe) GEM series coaxial detector system of both P-and N-type. The resolution (FWHM) of the detector system is 1.8 keV for gamma-ray energy of 1.33 MeV of ^{60}Co and a nominal efficiency of 38 %.



Figure 16: Marinelli beaker filled with crude oil and sealed

Acquisition of the gamma spectrum was done for 24 hours (86400 s) using an ORTEC gamma spectroscopy system. Figure 17 presents the detector-beaker configuration.



Figure 17: Detector-Beaker configuration

To account for background contribution to the sample spectrum, an empty sample container was counted for 86400 seconds (24 hours) as well. The detector system manufactured by AMETEK ORTEC, U.S.A was used. With embedded Multichannel Analyser controls, advanced spectrum analysis functions, automation for routine operations, quality control and security, the DSPEC LF was interfaced to a computer as illustrated in Figure 18, and the data evaluated using the Gamma Vision software package.



Figure 18: DSPEC LF MCA -To- computer configuration

Chapter Summary

This chapter discussed how the crude oil samples were obtained, the geographical locations where the samples were obtained and the different spectroscopic procedures employed. The experimental procedures for Laser-Induced Fluorescence, Energy-Dispersive X-Ray Fluorescence and Gamma-Ray Spectrometry were also expounded.

CHAPTER FOUR

RESULTS AND DISCUSSION

Introduction

This chapter describes and discusses the results obtained from the measurements conducted on the various crude oils, the mathematical processing algorithms employed to process and extract hidden information in the spectral data and the use of principal component analysis to assess the spectra variance. The results obtained in measuring the fluorescence spectra of the samples using LIF will be discussed. Additionally, sulphur concentration results determined using XRF and radioactivity concentration using gamma spectrometry will be presented and discussed.

Fluorescence Emission of Crude Oil Samples

The unprocessed laser-induced fluorescence (LIF) spectra obtained from each of the four samples, JF, TF, SF 1 and SF 2, are shown in Figure 19. These fluorescence spectra were as a result of the excitation of the crude oil samples with a 405 nm continuous wave laser source. The fluorescence peaks were observed near 500 nm and 560 nm with shoulder fluorescence emission peaking around 620 nm and 650 nm. The fluorescence intensities for TF, SF 1 and SF 2 crude oil samples appear to be closer to each other as compared to the crude oil sample from JF. This is in agreement with a previous study (El-Hussein & Marzouk, 2015).

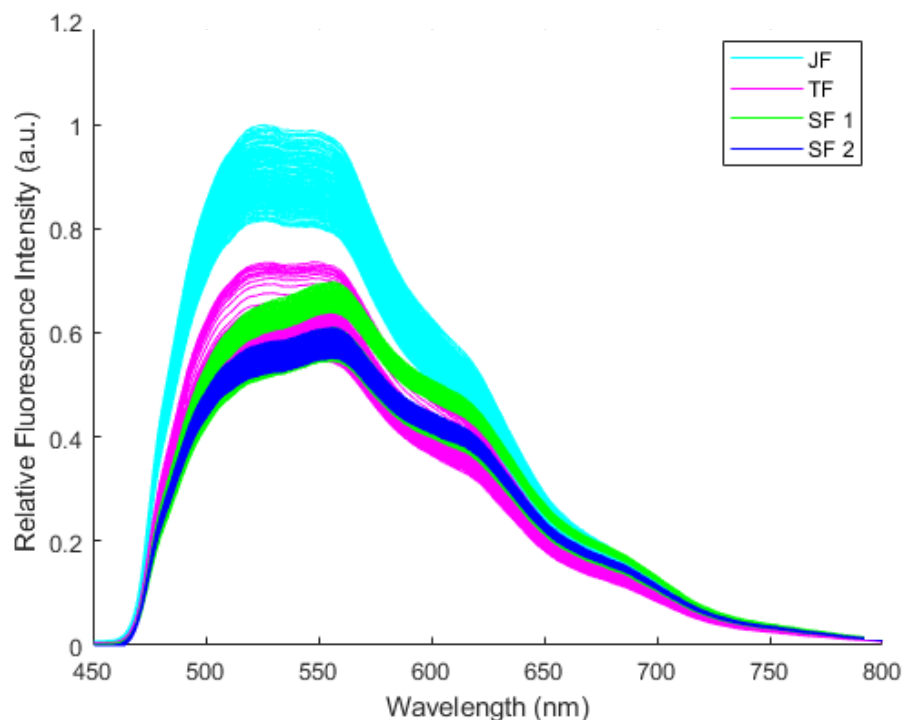


Figure 19: Unprocessed relative fluorescence spectra of all the crude oil samples, JF, TF, SF 1 and SF 2 from the four oil wells showing the dominating spectral signatures

These fluorescence emissions are affected by several factors, some of which will affect the emission behaviours observed. A wide variety of molecules or ions, act as fluorescence quenchers; that is, they decrease the intensity of the emission with oxygen being a typical example (Lakowicz, 2006). Fluorescence quenching can also occur through a variety of nonmolecular mechanisms, such as attenuation of the incident light by the fluorophore (fluorescent chemical compounds that can re-emit light upon excitation) and other absorbing species (Lakowicz, 2006). Other factors may include energy transfer (Fluorescence Resonance Energy Transfer), the rigidity of the local environment, changes in radiative and non-radiative decay rates and the kind of solvents used (El-Hussein & Marzouk, 2015; Lakowicz, 2006).

The fluorescence spectra were normalised using the maximum normalisation method to get rid of unwanted spectral variations as a result of the scattering of light from the samples. Figure 20 shows the average normalised fluorescence spectra obtained for each sample.

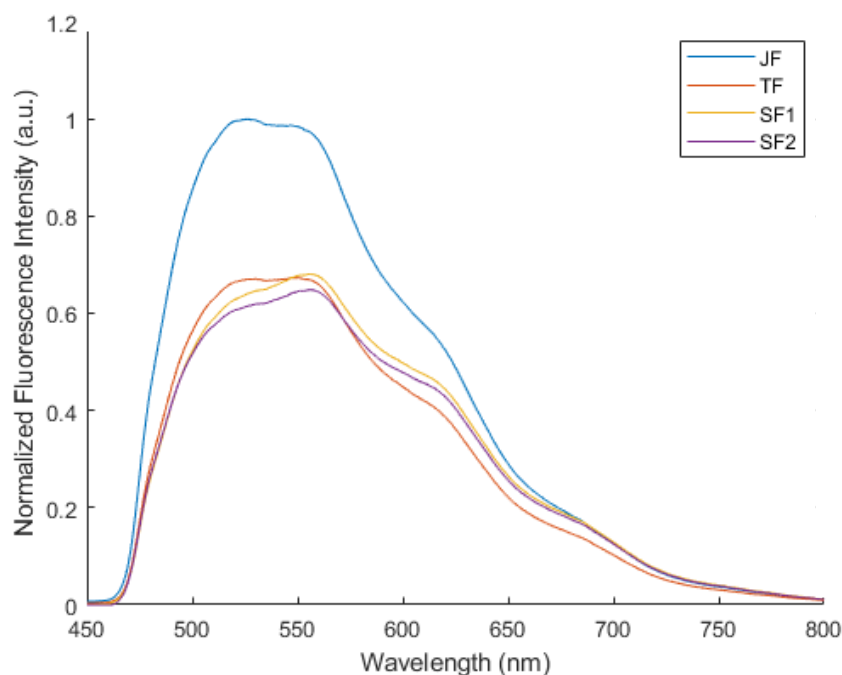
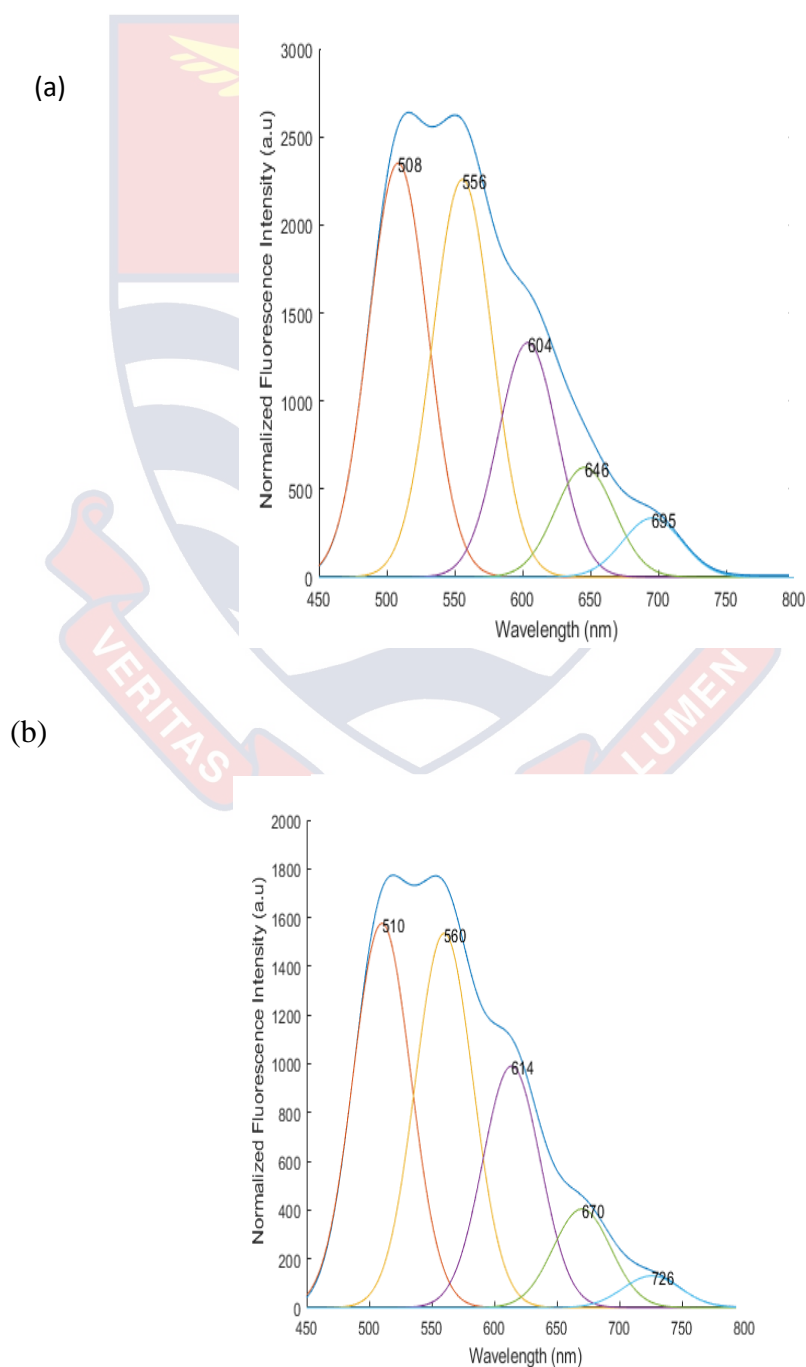


Figure 20: Average normalized fluorescence spectra from four crude oil samples

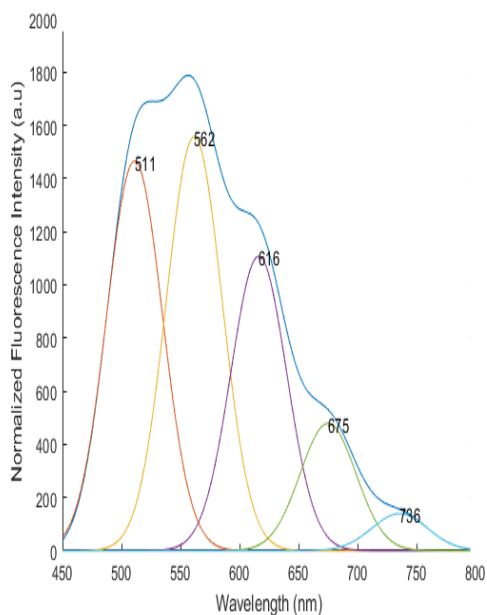
The fluorescence spectra profile observed for TF, SF 1 and SF 2 oil samples fit the general characteristics of light oils with low specific gravities and fluorescence band intensities (El-Hussein & Marzouk, 2015). JF is characterised by a higher fluorescence band intensity, which implies that crude oil from JF is heavier than those from TF, SF 1 and SF 2 (El-Hussein et al., 2015; Schultze, Lemle & Lömansröben, 2004).

Fluorescence Spectra Deconvolution of Crude Oil Samples

The spectrum for each sample was deconvolved using the Gaussian Function Fitting method to extract information about the hidden fluorescence peaks. Figure 21 is a composite graph showing the deconvoluted fluorescence spectra of the four oil wells, JF, TF, SF 1 and SF 2. These fits were obtained with correlation coefficient (r^2 value) above 0.99.



(c)



(d)

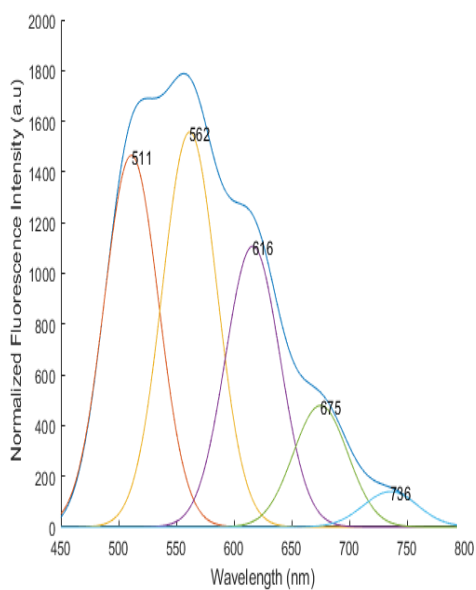


Figure 21: Deconvoluted fluorescence spectra of (a) JF, (b) TF (c) SF 1 and (d) SF 2 showing the hidden peaks

The deconvoluted fluorescence spectra consisted of Gaussian components observed at different peak wavelengths and intensities. From Figure 21, it can be observed that the significant fluorescence peaks occur within a range of 510 - 750 nm. These fluorescence peaks are similar to other fluorescence emission results obtained for crude oils observed by other researchers (El-Hussein & Marzouk, 2015; Steffens et al., 2011; Schultze, Lemle & Lömannsröben, 2004; Asiamah et al., 2013). The similarities in peak wavelengths for SF 1 and SF 2 suggest that they possess similar fluorophores and could have the same molecular characteristics since they are both drilled within the same field. The peak wavelengths and intensities of the deconvoluted fluorescence spectra are shown in Table 5.

Table 5: Results of Deconvoluted Fluorescence Spectra for the Crude Oil samples from all four (4) Oil Wells

PEAKS	JF		TF		SF 1		SF 2	
	λ (nm)	I (a. u.)						
1	508	2350	510	1576	511	1465	511	1438
2	556	2257	560	1535	562	1557	562	1495
3	604	1331	614	990	616	1107	616	1075
4	645	623	670	404	675	479	675	468
5	695	335	726	130	736	139	736	138

The differences in the peak wavelengths suggest that the crude oil samples from oil wells JF, TF and SF, have different fluorophore compositions and do not have the same molecular characteristics. (El-Hussein & Marzouk, 2015; Steffens et al., 2011).

The average peak wavelength values of the deconvoluted fluorescence spectra for the oil samples are shown in Table 6. These average peak wavelengths provide, for the first time, the standard deconvoluted peak wavelength range, 510-750 nm, indicating the specific peak wavelengths range at which fluorescence is occurring. The peak wavelengths also suggest that there are five (5) main different fluorophores responsible for fluorescence emission in the crude oil samples JF, TF and SF.

Table 6: Average Peak Wavelength Values of Deconvoluted Fluorescence Spectra for crude oil samples from JF, TF, SF 1 & SF 2 Oil Fields

Peaks	Wavelength (nm)
1	510.00 ± 1.41
2	560.00 ± 2.83
3	612.50 ± 5.74
4	666.50 ± 13.87
5	723.25 ± 19.41

Data behind ± for this work are standard deviations

Principal Component Analysis (PCA) of the Fluorescence Spectra obtained from Crude Oil Samples

Principal Component Analysis (PCA) was worth exploring to find the variations that occurred in the fluorescence spectra to allow for more insight into what was different between JF, TF, SF 1 and SF 2. The PCA simplified the large data set obtained from the fluorescence measurements by reducing the dimensionality and extracting the principal component coefficients and the eigenvalues of the covariance matrix of the data. Each spectrum was then plotted as a single point in PC space based on the variance across the entire data set.

Figure 22 shows the Scree plot containing the eigenvalues of the covariance matrix of the fluorescence spectra from the crude oil samples. It determines the number of factors to retain in the exploratory analysis (EA) or which principal components to keep in a principal component analysis (PCA).

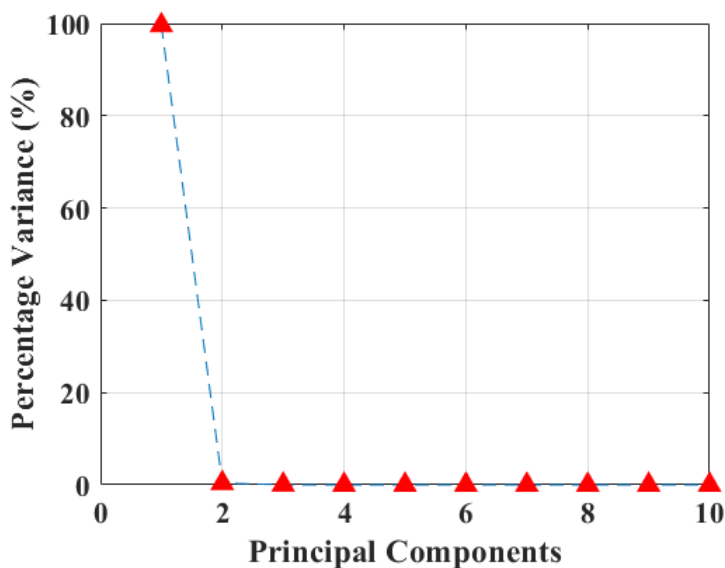


Figure 22: Number of Principal Components and their contribution to the variation in data set explained percentagewise

It has been suggested that the point where the scree plot levels off and flattens, is where the best possible principal components can end (Martinez & Martinez, 2005; Opoku-Ansah, 2016) and also according to the amount of explained variance of the eigenvalue. So, two principal components (PCs) were selected to represent the whole data. The two PCs (PC1 and PC2) preserved the maximum variance in the fluorescence spectra. Out of 99.97 % discrepancy in the fluorescence spectra, PC1 contributed 99.59 % and PC2 0.38 %.

The loadings or coefficient plot is shown in Figure 23. It is made up of the coefficients of the principal component (PCCs). The rows of the principal components correspond to the wavelengths while the columns correspond to the principal components.

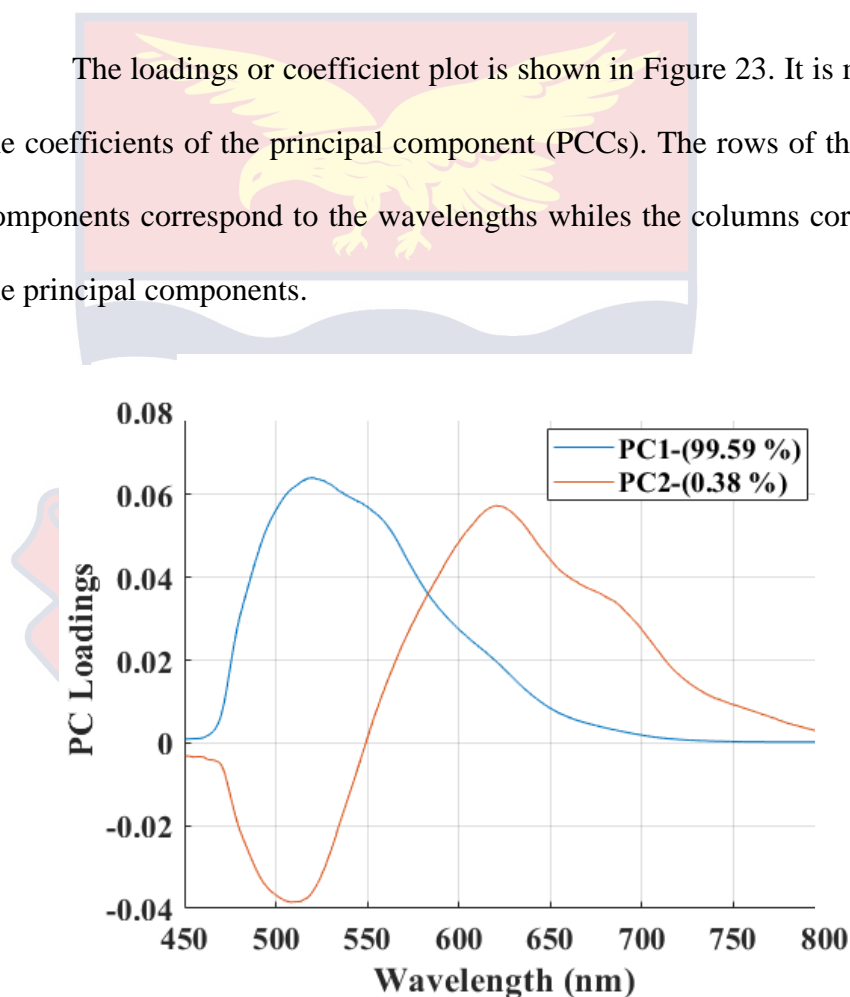


Figure 23: Loadings Plot from the PCA of the LIF spectra giving information about the significant sources of variation in the data

The loadings plot shows the regions where the differences and similarities between the fluorescence spectra can be observed within 450 nm – 800 nm range. It also reflects the unique grouping of the four (4) crude oil samples. This

plot helps to show the trend of the observations. From the plot, the significant differences in the fluorescence spectra are set to occur within 470 – 570 nm range.

The Score plot in Figure 24 shows the clustering of the fluorescence spectra in PC space based on the two significant PCs selected and gives the variance across the entire data set.

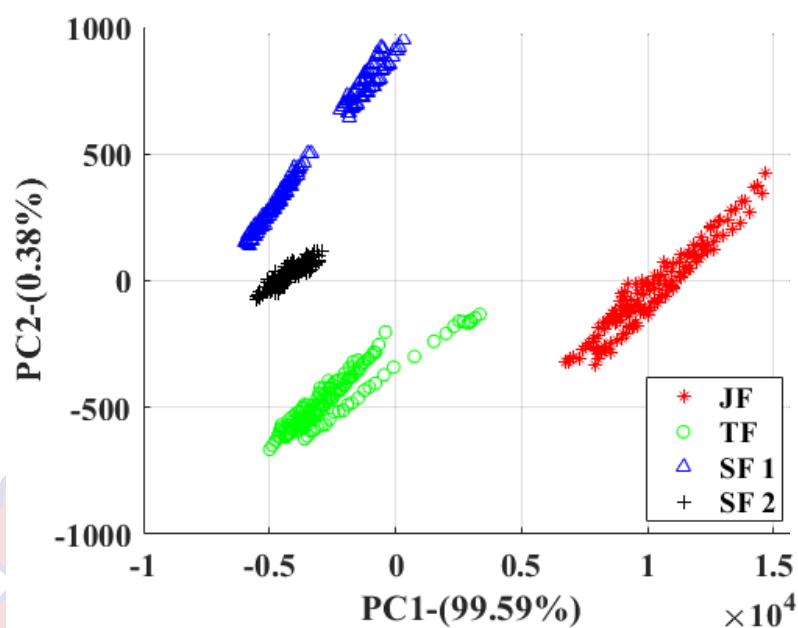


Figure 24: Score Plot for PC1 and PC2 from Principal Component Analysis of the LIF spectra obtained from the four crude oil samples, JF, TF, SF 1 and SF 2

Sample JF was separated from TF and SF along PC1, which suggests that crude oil from JF, is heavier than those from TF and SF. The negative loadings for PC2 show a trough, which explains the differences observed in the fluorescence spectra of JF, TF, SF 1 and SF 2 samples in the Score plot. It is therefore feasible to report that due to the different geological sources from

which the crude oil samples were obtained, crude oil composition varied from oil field to oil field. The PCA has shown that with only two PCs, the LIF of the crude oils from these four different wells can be discriminated.

Hierarchical Clustering Analysis (HCA) of the Fluorescence Spectra

Hierarchical Clustering Analysis (HCA) works by generating a data hierarchy leading to the formation of a dendrogram. Figure 25 shows the dendrogram of the LIF spectra of the four crude oil samples.

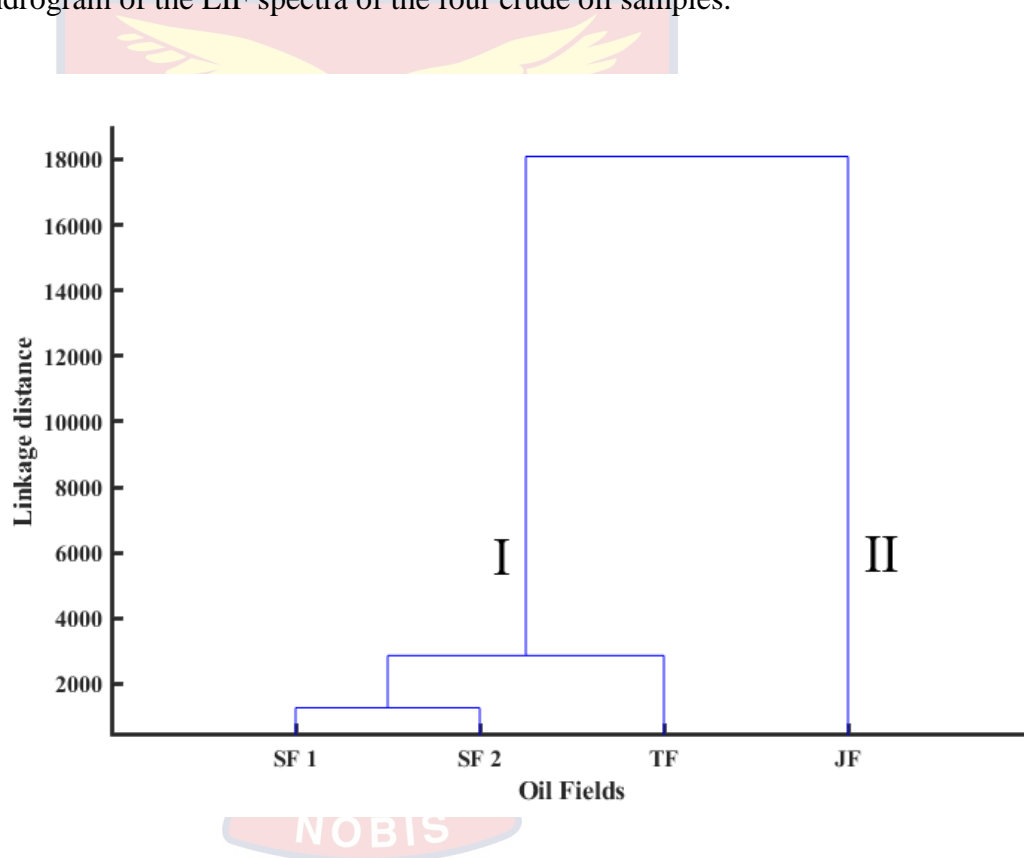


Figure 25: Dendrogram of the Laser-Induced Fluorescence spectra of the four crude oil samples from JF, TF, and SF.

The cluster labelled I consist of SF 1, SF 2 and TF, while cluster II is made up of JF. The HCA has been able to discriminate between the crude oil samples by calculating the linkage or Euclidean distance between JF, TF, SF 1 and SF 2 and classifying them into two major clusters. The shorter linkage

distances observed in cluster I suggest that TF and SF are lighter oils since they form under one cluster. Also, JF separates from the rest of the samples with a longer linkage distance, which suggests that JF could be heavier in molecular composition. The ability of the HCA to discriminate between the crude oil samples suggests that HCA can also be used to classify the crude oils from the four different oil wells.

Linear Discriminant Analysis (LDA)

Figure 26 is a composite graph showing the confusion matrix of the LIF spectra trained and test sets using the LDA model from the four crude oil samples. The confusion matrix provides a summary of what the discriminant function has done for each class. Each row shows the correct label, and each column shows one type of prediction. Two hundred (200) LIF spectra were used for the test set. The classification results for both trained and test sets were 100 % using the LDA. There is no misclassification of the crude oil samples based on their LIF spectra.

(a)

True Class	JF	97			
	SF 1		94		
	SF 2			106	
	TF				103
		JF	SF 1	SF 2	TF
		Predicted Class			

(b)

True Class	JF	53			
	SF 1		56		
	SF 2			44	
	TF				47
		JF	SF 1	SF 2	TF
		Predicted Class			

Figure 26: Confusion Matrix for the LIF (a) Trained set and (b) Test set of crude oil samples for the LDA model

Sulphur Concentration

The sulphur concentration results obtained from crude oil samples from the four oil wells JF, TF, SF 1 and SF 2 using EDXRF are shown in Table 7.

Table 7: Sulphur Concentration Levels of Crude Oil samples

Samples	Sulphur wt %
JF	0.281
TF	0.275
SF 1	0.188
SF 2	0.123

The sourness or sweetness of crude oil refers to its sulphur content (Appenteng et al., 2012). Crude oils with low sulphur content are commonly called sweet. Globally, sulphur levels are estimated at *0.1 wt % to 0.5 wt %* for sweet and *1.0 wt % to 3.3 wt %* for sour crude (UNEP/PCFV, 2009; El- Hussein & Marzouk, 2015). Generally, the lower the sulphur content, the lower its specific gravity (Khuhawar, Aslam & Jahangir, 2012).

The SF 1 and SF 2 recorded lower sulphur concentrations of 0.188 wt % and 0.123 wt % respectively, suggesting that these oils have very low specific gravities (Khuhawar, Aslam & Jahangir, 2012). These are therefore very light and sweet as compared to JF and TF that recorded the higher sulphur concentration. Similarities in their geochemical properties suggest that they could be sharing the same marine origin (source sedimentary rock) as observed in the sulphur levels for JF and TF (0.281 and 0.275 wt % respectively).

Radionuclides from the Crude oils

The gamma energies of the radionuclides of interest were identified because of the processed gamma signals stored in the channels allocated by the DSPEC LF Multichannel Analyser (MCA). There was the need to perform an efficiency calibration which has been presented in Figure 27. Below 2.3 of the logarithmic energy, the detector readings are considered not meaningful since the detector does not record all the gamma rays emitted by the sample.

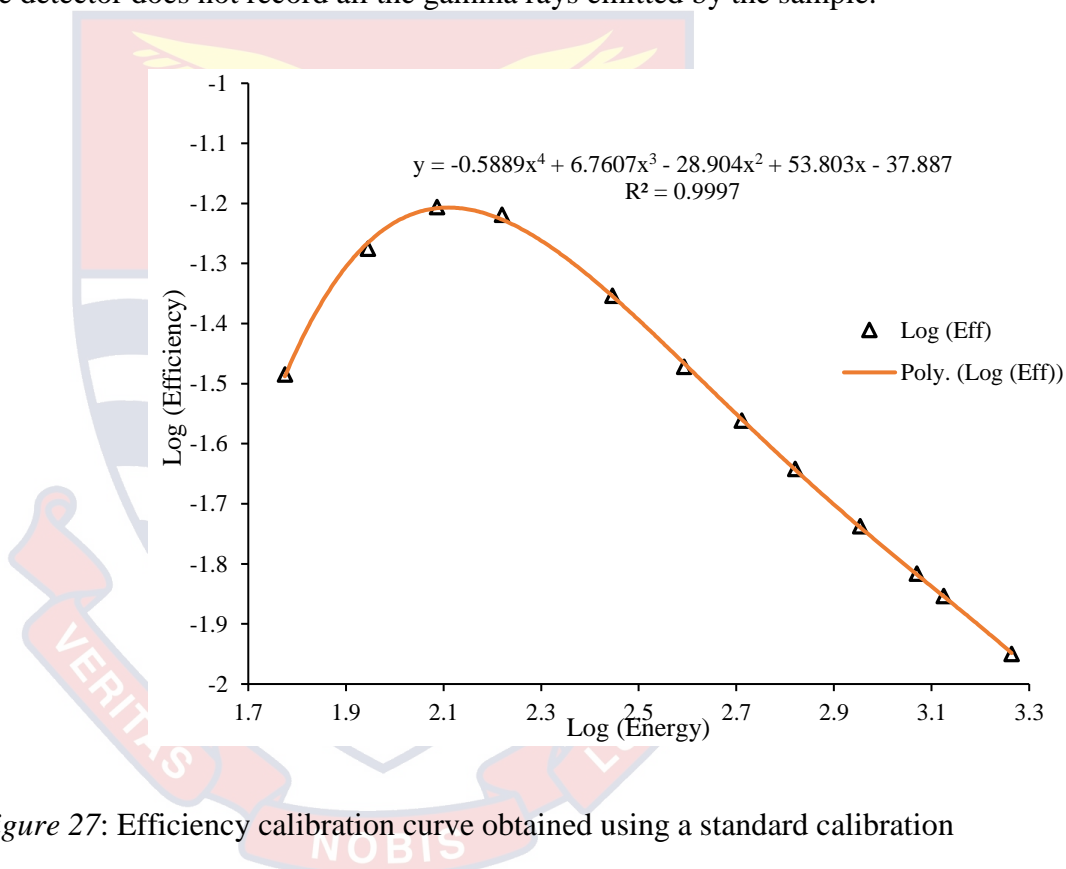


Figure 27: Efficiency calibration curve obtained using a standard calibration source with radionuclides (^{60}Co) of known activity

Figure 28 shows the energy calibration, which is a relationship between the channels selected by the MCA and the gamma-ray intensity.

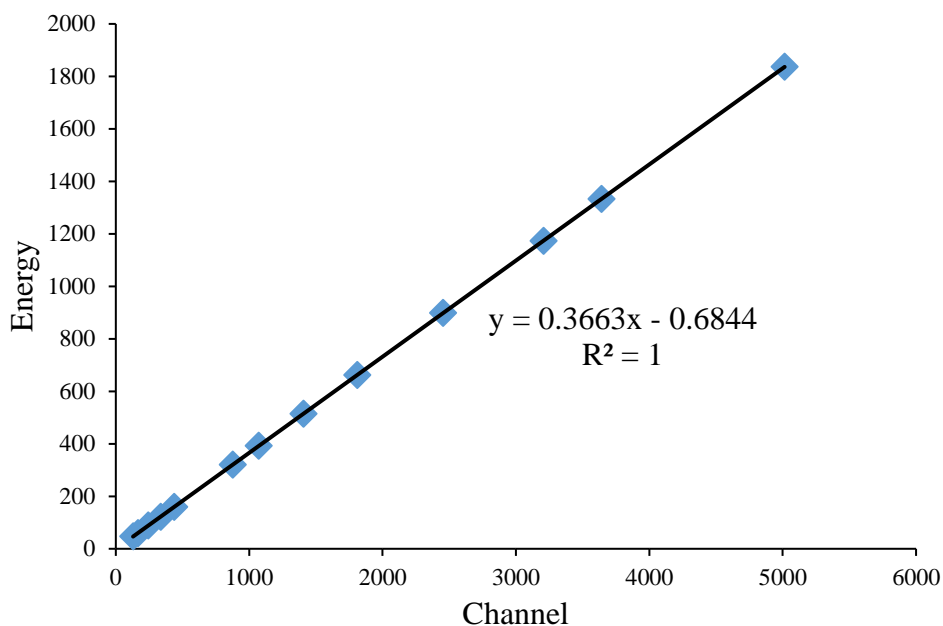


Figure 28: Energy calibration graph showing the relationship between the channels and their gamma intensities

The r-squared value obtained from the bivariate regression analysis is 1. Examining how well the number of channels could predict the energy or intensity of the gamma-ray, 100 % of the variance in energy is expected from the channels since this is a strong relationship (Cohen, 1988). Thus, for each unit increase of energy, the number of channels receiving the signals increase correspondingly. The results of the radioactivity concentrations of radionuclides ^{226}Ra , and ^{232}Th from JF, TF, SF 1 and SF 2 are summarised in Table 8.

Table 8: Activity Concentrations of ^{226}Ra , and ^{232}Th from JF, TF and SF Compared to the IAEA Basic Safety Standards (BSS) Exemption Level, 1×10^1 (Bq/g)

Crude oil samples	Nuclide Activity (Bq/g) $\times 10^{-3}$	
	Ra-226	Th-232
JF	3.37	0.84
TF	3.98	1.45
SF 1	5.56	0.74
SF 2	3.22	1.04

Presently, no research work has been conducted on NORMs in crude oil samples from JF, TF, SF 1 and SF 2. The results obtained for ^{226}Ra , ^{232}Th and ^{40}K in the samples were very low in activity concentration per the International Atomic Energy Agency (IAEA) Basic Safety Standards (BSS) exemption levels for Radium-226 (^{226}Ra) and Thorium-232 (^{232}Th).

However, it is worth mentioning that although the activity concentrations of Radium-226 (^{226}Ra) and Thorium-232 (^{232}Th) fell within the accepted IAEA Basic Safety Standards, SF 1 recorded the highest activity concentration of 5.56 Bq/L for Radium-226 (^{226}Ra) while SF 2 recorded the lowest activity concentration of 3.22 Bq/L. Crude oil composition may vary due to the differences in crude oil maturity and can be determined based on their Vanadium-Nickel (V/Ni) ratios (Appenteng et al., 2012).

Activity concentration of Potassium-40 (^{40}K) obtained in this work is very low per the IAEA Basic Safety Standards (BSS) for activity concentrations of radionuclides of natural origin as presented in Table 9.

Table 9: K-40 Activity Concentration obtained in this work compared to IAEA Basic Safety Standards (BSS) Activity for Radionuclides of Natural Origin, 10 Bq/g

Crude oil sample	Activity Concentration K-40 (Bq/L)	Activity Concentration K-40 (Bq/g)
JF	48.15	0.04815
TF	30.88	0.03088
SF 1	44.58	0.04485
SF 2	39.49	0.03949

Crude oil composition varies significantly for each oil well due to the differences in their geological origins (Appenteng et al., 2012; Asiamah et al., 2013). The distinct differences can be observed from the activity concentrations of radionuclides obtained for each sample.

The results obtained using gamma spectrometry in analysing the activity concentrations showed that the activity concentrations of the radionuclides, ^{226}Ra , ^{232}Th and ^{40}K , are very safe to handle. Handling these crude oils during the refinery processes, transportation, and research would not pose any health threat. They are very safe considering the International Atomic Energy Agency (IAEA) Basic Safety Standards for exemption levels.

Chapter Summary

In this chapter, results obtained from data analysed from crude oil samples from four disparate oil wells JF, TF, SF 1 and SF 2 using three spectroscopic methods; Laser-Induced Fluorescence (LIF), Energy-Dispersive

X-Ray Fluorescence (EDXRF) and Gamma-Ray Spectrometry have been presented and discussed. The unprocessed LIF spectra obtained from the four samples were normalized. Each of the normalized average fluorescence spectra was subjected to deconvolution to extract information about the hidden fluorescence peaks. Two unsupervised pattern recognition techniques (PCA and HCA) were used to identify and classify crude oils. A Linear Discriminant Analysis model generated from the PCA also classified the crude oil samples by generating a confusion matrix which specified the number of each observation into the four classes JF, TF, SF 1 and SF 2. Sulphur concentration levels determined in the crude oil samples using EDXRF showed that crude oil from all four oil wells JF, TF, SF 1 and SF 2 was sweet.

Finally, results of the radionuclides of interest (^{226}Ra , ^{232}Th and ^{40}K) from the crude oil samples analysed showed that their activity concentrations fell within the IAEA Basic Safety Standard Exemption levels. They can therefore be considered safe to handle and environmentally friendly.

CHAPTER FIVE

SUMMARY, CONCLUSIONS AND RECOMMENDATIONS

Overview

Due to the different geological sources of crude oil that Ghana has, the crude oil composition is expected to vary. Four (4) crude oil samples obtained from four different oil fields. Jubilee oil fields (JF), TEN oil fields (TF), Saltpond oil fields Well 2 (SF 1) and Well 4 (SF 2) in the coastal arches of Ghana have been studied. Three spectroscopic techniques: Laser-Induced Fluorescence (LIF), Energy-Dispersive X-Ray Fluorescence (EDXRF) and Gamma-Ray Spectrometry were used. This study sought to differentiate between Ghanaian crude oils using LIF as a fast and straightforward spectrochemical technique and to characterize Ghanaian crude oils and compare the outcome to results obtained from Energy Dispersive X-Ray Fluorescence and Gamma Spectrometry.

Summary

Laser-Induced Fluorescence (LIF), Energy-Dispersive X-Ray Fluorescence (EDXRF), and Gamma-Ray Spectrometry were used. The LIF spectra obtained for the samples showed five significant peaks within the spectral range of 510-750 nm, which is a characteristic of sweet and light crude oils with low specific gravities (or High API Gravity). The normalised LIF spectra for the samples were deconvolved to extract hidden fluorescence peaks observed in the fluorescence spectrum. From the four different geological zones from which they were obtained, JF, TF, SF 1 and SF 2 were observed to belong to five (5) main fluorescence spectra groupings with unique maximum peak

positions at (510.00 ± 1.41) nm, (560.00 ± 2.83) nm, (612.50 ± 5.74) nm, (666.50 ± 13.87) nm and (723.25 ± 19.41) nm. These dominating fluorescence bands reflect the various concentration levels of the different fluorophores present in the crude oil samples.

Principal Component Analysis (PCA) and Hierarchical Clustering Analysis (HCA) was used to ascertain the variations and similarities in the LIF spectra obtained. These two unsupervised pattern recognition techniques (PCA and HCA) identified cluster trends in the spectra data and classified JF, TF, SF 1 and SF 2 according to their geological locations based on the LIF spectra. Thus, PCA and HCA showed that all the crude oil samples belonged to different geological zones. Cluster II and III consist of TF (TEN oil field) and JF (Jubilee oil field). The Score plot of the PCA was further used to generate a Linear Discriminant Analysis (LDA) classification model, a supervised pattern recognition technique that can quickly identify and classify unknown crude oil samples. The classification results show that LDA can be used to determine the crude oil samples and their locations based on the LIF spectra obtained.

The Energy Dispersive X-Ray Fluorescence technique was used to identify and quantify the Sulphur content in the crude oil samples. It was able to characterise the samples based on their Sulphur concentrations. Although the results obtained showed that TEN oil field had the highest Sulphur concentration, all the crude oil samples investigated in this work can be classified as *sweet crude*.

Radioactivity concentrations of the samples were determined for the following Naturally Occurring Radioactive Materials (NORMs) using a

Gamma-ray Spectrometer. ^{226}Ra (Radium-226), ^{232}Th (Thorium-232) and ^{40}K (Potassium-40). The average activity concentration results obtained for ^{226}Ra , ^{232}Th , and ^{40}K were 4.03 ± 1.07 Bq/L, 1.02 ± 0.31 Bq/L and 40.84 ± 7.54 Bq/L respectively. In this work, the radioactivity concentration values obtained for crude oil samples from Jubilee, TEN, and Saltpond oil fields fall within the Basic Safety Standards (BSS) of the International Atomic Energy Agency (IAEA).

Conclusions

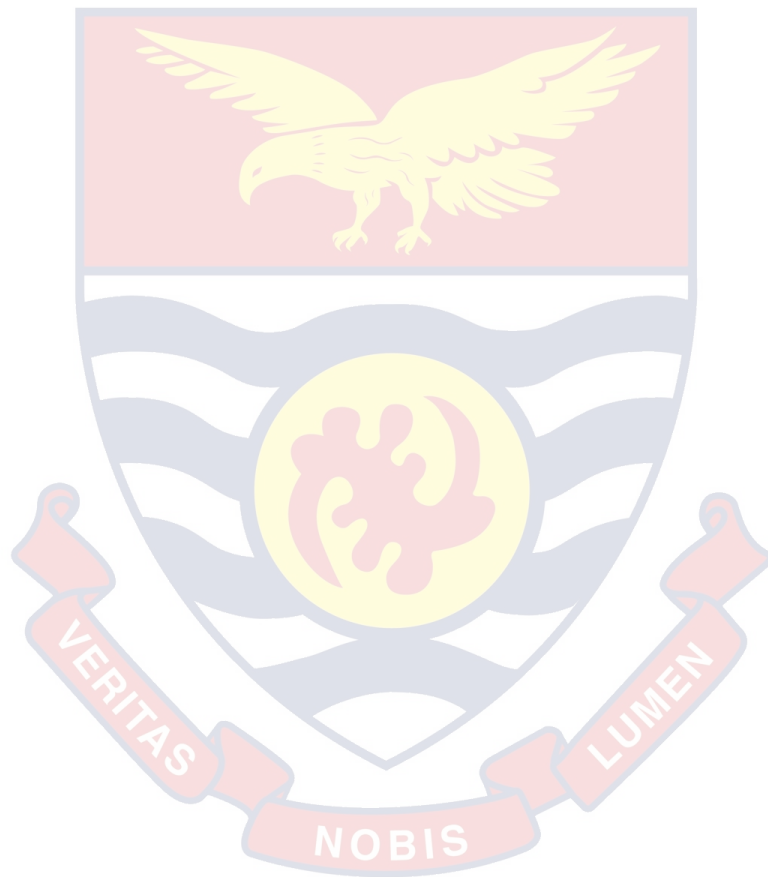
Laser-Induced Fluorescence coupled with Principal Component Analysis (PCA), Hierarchical Clustering Analysis (HCA) and Linear Discriminant Analysis (LDA) was used as a fast and straightforward spectrochemical analytical method to effectively characterise crude oil samples from Jubilee, TEN and Saltpond oil fields in Ghana.

Results obtained from Energy Dispersive X-Ray Fluorescence (EDXRF) measurement classified the four (4) crude oil samples as sweet. This further suggests that crude oil from Jubilee (0.281 wt %), TEN (0.275 wt %) and Saltpond oil fields (0.123-0.188 wt %) are of good quality since they fall within the globally accepted sulphur levels as observed in the samples investigated.

Finally, three naturally occurring radioactive materials (NORMs) ^{226}Ra , ^{232}Th , and ^{40}K were identified across the Jubilee, TEN and Saltpond oil fields. Their radioactivity concentrations were acceptable within the IAEA BSS Exemption Levels and pose no health and environmental threat to all persons who come into contact with them.

Recommendations

It is recommended that state-owned corporations, petroleum research institutes and laboratories adopt the use of the LIF technique to identify and classify oil samples. It is also recommended that the possibility of using this technique to detect adulteration of crude oils be investigated based on their locations.



REFERENCES

- Abdalla, S.S. (2015). *Determination of Hydrogen Content of Petroleum Products from Tema Oil Refinery Using Neutron Backscatter Technique*. MPhil Thesis. University of Ghana, Legon. Retrieved from: <https://ugspace.ug.edu.gh>.
- Adipah, S. (2019). Introduction of Petroleum Hydrocarbon Contaminants and its Human Effects. *Journal of Environmental Science and Public Health*, 3: 001-009.
- American Society for Testing and Materials [ASTM]. (2003). *Standard Test D4294 for Sulphur in Petroleum and Petroleum Products by Energy Dispersive X-ray Fluorescence Spectroscopy*. American National Standard.
- American Society for Testing and Materials [ASTM]. (1993). Standard Test E579-84, Test Method for Limit of Detection of Fluorescence of Quinine Sulfate. *Annual Book of ASTM Standards*. (Vol. 14.01). Philadelphia, PA.
- Amuah, C.L.Y., Eghan, J.M., Anderson, B., Adueming, P.O.-W., & Opoku-Ansah, J. (2017). *Laser-Induced Fluorescence in combination with Multivariate analysis classifies anti-malarial herbal plants*. Paper presented at the Frontiers in Optics, Washington, D.C.
- Amuah, C.L.Y. (2020). *Spectroscopic Studies of Some Selected Anti-Malarial Herbal Plants Sample Combined with Multivariate Data Analysis*. PhD Thesis, Laser and Fibre Optics Centre (LAFOC), University of Cape Coast.
- Ante, J. (2013). *Petroleum Refining and Petrochemical Process*. Faculty of Chemical Engineering and Technology, University of Zagreb.

API Manual of Petroleum Measurement Standards, Chapter 11.1-1980, Volume XI/XII, Adjunct to ASTM D1250-80 and IP 200/80.

Appenteng, M.K., Golow, A.A., Carbov, D., Adomako, D., Hayford, M.S., Yamoah, A.K.Y., Saka, D., & Sarfa, D.K. (2012). *Multi-element analysis of Ghanaian crude oils by instrumental neutron activation analysis*. J Ramimal and Nucl Chem. 292:1197-1206.

Appenteng, M.K., Golow, A.A., Carbov, D., Nartey, V., Kaka, E.A., Salifu, M., & Aidoo, F. (2013). *Physicochemical characteristics of the jubilee crude oil*. Elixir Applied Chemistry. 54.

Audi, G., Bersillon, O., & Blachot, J. (2003). *The NUBASE evaluation of nuclear and decay properties* (PDF). Nuclear Physics A. 729(1): 3-128. Bibcode: 2003NUPhA.

Asiamah, F., Asamoah, J., Mfodwo, K., & Dasoveanu, L. (2013). *Handbook on oil and gas for journalists.: from the International Institute of ICT Journalism: Accra, Ghana*. ISBN: 978-9988-1-8452-0.

Ayoade, M.A. (2002). *Discussed offshore installation and pipelines*. Kluwer Law International, ISBN. 90-411-1739-3.

Balshaw-Biddle, K. (ed). (2000). *Subsurface monitoring using laser fluorescence*. Lewis Publishers, Boca, Raton.

Baumann, T., Haaszio, S., & Niessner, R. (2000). *Applications of a laser-induced fluorescence spectroscopy sensor in aquatic systems*. Water Res. 34: 1318-1326.

Bawazeer, K., & Zilouchian, A. (1997). *Prediction of Products Quality Parameters of Crude Fractioning Section of an Oil Refinery Using Neural Networks*. J. lit. Conf. Neural Netw. 1: 157-62.

- Bujewski, G., & Rutherford, B. (1997). *The Rapid Optical Screening Tool (ROST) Laser-Induced Fluorescence (LIF) System for Screening of Petroleum Hydrocarbons in Subsurface Soils*. Innovative Technology Verification Project Report, Las Vegas.
- BusinessGhana.(2018).
<https://www.businessghana.com/site/news/general/161574/Ghana-The-worlds-next-oil-hotspot>. Assessed 25th June 2019.
- Burke, W.J. (2019). *A robust and automated deconvolution algorithm of peaks in spectroscopic data*. Theses and Dissertations. 2657.
Retrieved from:<https://rdw.rowan.edu/etd/2657>.
- Brandriss, M.E. (2010). *Using High-Precision Specific Gravity Measurement to Study Minerals in Undergraduate Geoscience Courses*. Journal of Geoscience Education, V.58, n.3. P.155-165.
- Camagni, P., Colombo, G., Koechler, C., Pedrini, A., Omenetto, N., & Rossi, G. (1988). IEEE Trans. Geosc. Remote Sensing GE-26,22.
- Cohen, J. (1988). *Set Correlation and Contingency Table*. Sage Journals.
Retrieved from: <https://doi.org/10.1177/014662168801200410>.
- Collins, R.N., Saito, T., Aoyagi, N., Payne, T.E., Kimura, T., & Waite, T.D. (2011). *Applications of time-resolved laser fluorescence spectroscopy to the environmental biogeochemistry of actinides*. J. Environ. Qual. 40. 731-741.
- Daučík, P., Zidek, Z., & Kalab, P. (1998). *Determination of Sulphur Content in Fuels*. Chem. Papers 52(5), 667-670.
- Demtröder, W. (2013). *Laser spectroscopy: basic concepts and instrumentation*; Springer Science & Business Media.

- Downare, T.D., & Mullins, O.C. (1995). *Visible and Near-infrared Fluorescence of Crude Oils*. *Appl. Spectrosc* 49: 754-764.
- Edward, G. (2016). *Uranium: A discussion Guide*. Retrieved from: https://www.ccnr.org/nfb_uranium_3.html.
- El- Hussein, A., & Marzouk, A. (2015). *Characterization of Petroleum Crude Oils using Laser-Induced Fluorescence*. *J Pet Environ Biotechnol* 2015. 6:5.
- Ellingsen, L., & Fery-Forgues, S. (1998). *Application de la spectroscopie de fluorescence à L'étude du pétrole: le défi de la complexité*. *Revue de l'institut Français du Pétrole*. 53(2) : 201-216.
- Environmental Protection Agency [EPA], Research & Development, (1997). Retrieved from: <https://www.epa.gov/superfund/health/contaminants/radiations/pdfs/umtrcagu.pdf>.
- Evdokimov, I.N., & Losev, A.P (2007). *Chem Technol Fuel Oils*. 43: 140. Retrieved from: <https://doi.org/10.1007/s10553-007-0027-5>.
- Fisher, R.S. (1998). *Geologic and geochemical controls on naturally occurring radioactive materials (NORM) in oil & gas production*. American Petroleum Institute, Washington, D.C., API Bulletin E2, 45p.
- Frontasyeva, M.V. (2011). *Neutron activation analysis in the life sciences*. *Phys. Part. Nuclei* 42, 332-378.
- Garvin, S.M. (2011). *Letter to PADEP re Marcellus shale. 030711 (PDF)*. EPA.
- Ghana National Petroleum Corporation [GNPC]. (2009). *Exploration and Production history of Ghana*. Retrieved from :[https:// www.gnpcghana.com](https://www.gnpcghana.com).
- Haken, H., & Wolf, H.C. (2004). *Molecular Physics and Elements of Quantum*

Chemistry: Introduction to Experiments and Theory. Edition 2, Springer-Verlag Berlin, Heidelberg.

Heftmann, E. (2004). *Fundamentals and Applications of Chromatography and Related Differential Migration Methods*. Journal of Chromatography Library. Volume 69, Part B, Pages 519-1156.

Hercules, D.M., & Joyner, D.J. (1979). *Chemical bonding and electronic structure of B₂O₃, H₃BO₃ and BN : An ESCA, Auger, SIMS, and SXS Study*. J. Chem. Phys. 72, 1095.

Hook, M. (2009). Licentiated Thesis, global energy systems, Department for Physics and Astronomy, Uppsala University, Uppsala, pp 3-13.

Hollas, J.M. (2004). *Modern Spectroscopy* (4th Ed): John Wiley & Sons. ISBN 0-470-84416-7.

Hotelling, H. (1933). Analysis of complex statistical variables into principal components. *Journal of Educational Psychology*, 24(6), 417.

Howley, J.R., & Robbins, C. (1967). *Radiation hazards from X-ray diffraction equipment, Radiology Health Data and Reports*, Vol. 8, p.245.

IAEA, (1996). International Basic Safety Standards for Protection against Ionizing Radiation and the Safety of Radiation Sources, Safety Series No. 115, IAEA, Vienna.

Jackson, J.E. (1981). *Principal Components and Factor Analysis: Part II- Additional topics related to principal components*. Journal of Quality Technology, 13(1), 46-58.

Jacquelin, J. (2009). *Régressions et équations intégrales* [Online]. Retrieved from:<https://www.researchgate.net/.../14674814-Regressions-etequations-integrales.pdf>.

- Jenkins, R., & Haas, D.. (1973). *Hazards in the use of X-ray Analytical Instrumentation*. X-ray Spectrometry, Vol.2, No.3. John Wiley & Sons Ltd.
- Jolliffe, I.T. (1986). Principal Component Analysis and Factor Analysis. In *Principal Component Analysis* (pp. 115-128): Springer.
- Jolliffe, I.T. (2002). Choosing a subset of Principal Components or variables. *Principal Component Analysis*, 111-149.
- Jolliffe, I.T. (2011). *Principal Component Analysis*: Springer.
- Kpeglo, D., Mantero, J., Darko, E., Faanu, A., Amoateng, E., Manjon, G., Vioque, I., & Tenorio, R.G. (2019). *Assessment of natural radioactivity levels and associated radiological hazard in scale and sludge from Jubilee oilfield of Ghana*. *International Journal of Low Radiation*. 21. 143-157.
- Lachance, G.C.F. (1995). *Quantitative X-ray Fluorescence Analysis*, Wiley.
- Lakowicz, J.R. (1992). *Topics in Fluorescence Spectroscopy: Principles* (Vol.2): Springer Science & Business Media.
- Lakowicz, J.R. (1998). *Principles of Fluorescence Spectroscopy*: Springer Science & Business Media.
- Lakowicz, J.R. (2006). *Solvent and Environmental Effects*. In: *Principles of Fluorescence Spectroscopy*. Springer, Boston, MA. Retrieved from: https://doi.org/10.1007/978-0-387-46312-4_6.
- Lakowicz, J.R. (2013). *Principles of Fluorescence Spectroscopy*: Springer Science & Business Media.
- Lömannsröben, H.G., Roch, T., & Schultze, R.H. (1999). *Laser-Induced Fluorescence Spectroscopy for In situ Analysis of Petroleum Products and Biological oils in soils*. *J. Polycyclic Aromatic Compounds* (Vol. 13).

<https://doi.org/10.1080/10406639908020561>.

Martinez, W.L., & Martinez, A.R. (2005). *Exploratory Data Analysis with MATLAB*. Computer Science and Data Analysis Series, Chapman & Hall/CRC.

Martinez, J.F., Villasenor, R., Rios, R., & Espinosa, C.F. (2004). Springer Science & Business Media, Inc.

McIntyre, S.M., Ma, Q., Burritt, D.J., Oey, I., Gordon, K.C., & Miller, S.J.F. (2020). *Vibrational spectroscopy and chemometrics for quantifying key bioactive components of various plum cultivars grown in New Zealand*. J. Raman Spectrosc. 1-15: John Wiley & Sons, Ltd.

Nave, C.R. (2020). Gaussian distribution function [Online]. Available : <http://hyperphysics.phy-astr.gsu.edu/hbase/Math/gaufcn.html>.

Opoku-Ansah, J. (2016). *Optical Studies and Characterization of Plasmodium Falciparum Infected Human Red Blood Cells*. Ph.D. Thesis, University of Cape Coast.

Ozaki, Y., McClure, W.F., & Christy, A.A. (2006). *Near-infrared spectroscopy in food science and Technology*: John Wiley & Sons, Ltd.

Pavia, L.D., Lampman, G.M., Kriz, G.S., & Vyvyan, A.J. (2008). *Introduction to Spectroscopy*. Edition 4, illustrated, Cengage Learning.

Pedersen, M. (2011). *Propagation of Shocks to Food and Energy Prices: An International Comparison*. Central Bank of Chile.

Perez, R., Ineichen, K.M., Kmiecik, M., Chain, C., George, R., & Vignola, F. (2002). *A New Operational Satellite-to-Irradiance Model*. Solar Energy 73,5, pp. 307-317.

Praider, B., Largeau, C., Derenne, S., Martinez, L., & Bertrand, P. (1990).

Chemical basis of fluorescence alteration of crude oils and kerogens.

Microfluorimetry of oils and their fractions. Org Geochem 16: 451-460.

Qasim, M., Ansari, T.M., & Hussain, M. (2016). *Physicochemical characteristics of Pakistani used engine oils.* Journal of Petroleum Technology and Alternative Fuels. Retrieved from: <https://doi.org/10.5897/JPTAF.2015.0121>.

Rayner, D.M., & Szabo, A.G. (1978). Fluorescence of Quinine Sulfate. *Annual Book of ASTM Standards.* Appl. Opt. 17, 1624.

Robert, R., Roussel, J., & Boulet, R. (1995). *Characterization of crude oil and petroleum fractions.* Journal of petroleum refining. 1:39-84, pp. 453-469.

Sauer, M., Hofkens, J., & Enderlein, J. (2012). *Handbook of Fluorescence Spectroscopy and Imaging: From Ensemble to Single Molecules.* 1st Edition. Anal Bioanal Chem, Wiley-VCH.

Savitzky, A., & Golay, M.J.E. (1964). *Smoothing and Differentiation of Data by Simplified Least Square Procedures.* Anal. Chem. 36: 1627-1639.

Schade, W., Bublitz, J., Helbig, V., & Nick, K.P. (1992). *Time-Resolved Laser-Induced Fluorescence Spectroscopy for Diagnostics of Oil- Pollution in Water.* In: Werner, C., Klein, V., & Weber, K. (Eds). Springer, Berlin, Heidelberg. https://doi.org/10.1007/978-3-642-50980-3_8.

Schultze, R., Lemle, M., & Löhmannsröben, H.G. (2004). *Laser-Induced Fluorescence (LIF) Spectroscopy for the In situ analysis of petroleum product contaminated soils.* Springer, Heidelberg, pp. 79-98.

Shakir, I.K., & Qasim, M.A. (2015). *Extraction of Aromatic Hydrocarbons from Lube Oil Using Different Co-Solvent.* Iraqi Journal of Chemical and Petroleum Engineering. Vol. 16. No.1 (79-90). ISSN: 1997-4884.

- Shawky, S., Amer, H., Nada, A.A., El-Maksoud, Abd., & Ibrahiem, N.M. (2011). *Characteristics of NORM in the oil industry from the Eastern and Western deserts of Egypt*. Applied Radiation and Isotopes 55, 135-139.
- Smith, K.P., Blunt, D.I., Arnish, J.J., Williams, G.P., Pflingston, M., Herbert, J., & Haffendem, R.A. (1999). *An Assessment of the Disposal of Petroleum Industry NORM in Nonhazardous Landfills*, Final Report, Fossil Energy, National Petroleum Technology Office, U.S. Department of Energy, Tulsa, Oklahoma, U.S.A.
- Smith, T.B. (2003). *Deconvolution of Ion velocity distributions from Laser-Induced Fluorescence Spectra of Xenon Electrostatic Thruster Plumes*. PhD Dissertation, Aerospace Engineering, University of Michigan.
- Steffens, J., Landulfo, E., Courrol, L.C., & Guardani, R. (2011). *Application of Fluorescence to the study of crude petroleum*. Journal of Fluorescence 21: 859-864.
- Subhash, N., & Mohanan, C.N. (1995). *Remote detection of nutrient stress in groundnut plants by deconvolution of laser-induced fluorescence spectra*. International Geoscience and Remote Sensing Symposium (IGARSS). 3. 2323-2325. (Vol.3). 10. 1109/IGARSS.
- Svanberg, S. (2012). *Atomic and Molecular Spectroscopy: basic aspects and practical applications (Vol. 6)*: Springer Science & Business Media.
- Takumi, S., Lukman, S., Aoyagi, N., Takaumi, K., & Nagasaki, S. (2012). *Speciation of Eu³⁺ bound to humic substances by time-resolved laser fluorescence spectroscopy (TRLFS) and parallel factor analysis (PARAFAC)*. Geochimica et Cosmochimica Acta. 88. 199-215.
- Tamrakar, P.K. (2000). *Biomass and volume tables with species description for*

community forest management. No. 101, Ministry of Forest and Soil Conservation.

Tamrakar, P.K., & Pitre K.S. (2001). *Electrochemical determination of lead in gasoline*. Bulletin of Electrochemistry. 16(12): 537-8.

UNEP/PCFV, (2009). *Worldwide Sulphur levels in diesel fuel*: Retrieved from:<http://www.kosmosenergy.com/ghana.html>.

United States Geological Survey [USGS]. (1999). *Naturally Occurring Radioactive Materials (NORM) in Produced Water and Oil- Field Equipment*. An Issue for the Energy Industry. Fact Sheet 142-99.
<https://doi.org/10.3133/fs14299>

Wang, G.J., Cheng, T.J., & Wang, D.Y. (2005). *Experimental study on trace element method in surface geochemical prospecting for oil and gas*. Petroleum Geology & Experiment. 27(5), 544-549.

White, G.J., & Rood, A.S. (1999). *5th Intern Petroleum Environmental Conf.*, University of Tulsa and Others, Albuquerque, N.M., U.S.A.